SPATIOTEMPORAL ANALYSIS OF EXTREME HEAT EVENTS

IN INDIANAPOLIS AND PHILADELPHIA FOR THE YEARS 2010 AND 2011

Kavya Urs Beerval Ravichandra

Submitted to the faculty of the University Graduate School
in partial fulfillment of the requirements
for the degree
Master of Science
in the Department of Geography,
Indiana University

July 2013

Accepted by the Faculty of Indiana University, in partial
fulfillment of the requirements for the degree of Master of Science.

_____

Daniel P. Johnson, Ph.D., Chair

_____

Jeffrey S. Wilson, Ph.D.

Master's Thesis
Committee

_____

Frederick L. Bein, Ph.D.

**ACKNOWLEDGEMENTS**

I would like to thank the members of my thesis committee, Dr. Daniel P. Johnson, Dr. Frederick L. Bein and Dr. Jeffrey S. Wilson.  I greatly appreciate their support, encouragement and teachings that helped me hone my research and academic skills.  I am grateful to my advisor Dr. Daniel P. Johnson for his guidance and knowledge that helped me stay on track.

I would like to thank Jeremy Webber for sharing his knowledge of remote sensing and GIS.  I am also thankful to Michelle Rigg, Austin Stanforth, Dr. Vijay Lulla, and Raymond Porter for their valuable inputs.  I would like to thank Joyce Haibe, Department of Geography for her valuable suggestions that helped me during my thesis and coursework.

My gratitude goes out to the Department of Geography, IUPUI for their financial support of my graduate work.

Lastly, I am indebted to my family for providing me constant support, advice and encouragement to complete my thesis and coursework.  I am also thankful to Patrick M. Ramsey for his moral support and encouragement which helped me greatly.

# ABSTRACT

Kavya Urs Beerval Ravichandra

SPATIOTEMPORAL ANALYSIS OF EXTREME HEAT EVENTS

IN INDIANAPOLIS AND PHILADELPHIA FOR THE YEARS 2010 AND 2011

Over the past two decades, northern parts of the United States have experienced extreme heat conditions.  Some of the notable heat wave impacts have occurred in Chicago in 1995 with over 600 reported deaths and in Philadelphia in 1993 with over 180 reported deaths.  The distribution of extreme heat events in Indianapolis has varied since the year 2000.  The Urban Heat Island effect has caused the temperatures to rise unusually high during the summer months.  Although the number of reported deaths in Indianapolis is smaller when compared to Chicago and Philadelphia, the heat wave in the year 2010 affected primarily the vulnerable population comprised of the elderly and the lower socio-economic groups.  Studying the spatial distribution of high temperatures in the vulnerable areas helps determine not only the extent of the heat affected areas, but also to devise strategies and methods to plan, mitigate, and tackle extreme heat.  In addition, examining spatial patterns of vulnerability can aid in development of a heat warning system to alert the populations at risk during extreme heat events.  This study focuses on the qualitative and quantitative methods used to measure extreme heat events.  Land surface temperatures obtained from the Landsat TM images provide useful means by which the spatial distribution of temperatures can be studied in relation to the temporal changes and socioeconomic vulnerability.  The percentile method used, helps to determine the vulnerable areas and their extents.  The maximum temperatures measured using LST conversion of the original digital number values of the Landsat TM images is reliable in terms of identifying the heat-affected regions.

Daniel P. Johnson, Ph.D., Chair

# TABLE OF CONTENTS

# LIST OF TABLES

# LIST OF FIGURES

**BACKGROUND**

Land use and land cover changes are driven by the development and expansion of urban areas. With the increase in urbanization, there is increase in ambient air temperatures and surface temperatures which cause the formation of heat islands. The impermeable urban materials used and the lack of porosity of such materials are some of the causes of increase in surface temperatures. Moreover, increased human activities in the urban areas increase the air temperatures, in contrast to the lower temperatures in the rural areas (Sabnis 2011). The loss of vegetation in the urban regions increases the surface albedo. The heat generated from vehicles, generators and other sources amplifies urban temperatures (Stone, Hess et al. 2010).

Voogt and Oke classified Urban Heat Islands (UHI) into two types: 1) The Urban Canopy Layer (UCL), and 2) The Urban Boundary Layer (UBL). The UCL is the layer between the surfaces to the mean building height where the temperature is influenced by the surface heat. The UBL is the layer above UCL where the temperature is influenced by the underlying sub-surface layer (Voogt and Oke 2003). Surface Urban Heat Island (SUHI) is measured in situ at meteorological stations, whereas, UBL heat island is measured using air-borne sensors where the temperature measurements are influenced by the atmospheric stability and turbulence. The remotely sensed UHI measurements have greater spatial variability than the air temperature measurements (Arnfield 2003).

Thermal remote sensing instruments measure the temperature of the SUHI indirectly, where surface emission and radiation are considered (Voogt and Oke 2003). The ambient air temperatures are recorded at meteorological stations located over limited areas such as sub-urban, rural regions or parks. The temperatures over residential areas and urbanized districts vary greatly from these regions. This biased estimation of air temperatures can be misleading since only the localized air

1

temperatures are measured.  The spatial distribution of surface temperature measurement using thermal remote sensors provides surface temperature variations over intra-urban areas to identify Urban Heat Islands (Kestens, Brand et al. 2011).

Extreme heat events in the urbanized regions of Midwestern US cities have increased over last few decades and it are likely to increase in severity in the future.(Patz, McGeehin et al. 2001)  A study by Stone et al., indicates that extreme heat events have intensified in the five-decade period, from 1956 to 2005, in large US cities, which is attributed largely due to sprawling.  Among the susceptible urban populations affected by extreme heat are the elderly, young children, and the poor; defined by race/ethnicity, and socio-economic class (Cutter and Finch 2008).  Various studies demonstrate the health risk associated with extreme heat in the urban areas.  In a study by (Johnson and Wilson 2009), the heat related deaths in Philadelphia 2003 were associated with poverty.  The results obtained by these studies provide a framework for future risk assessment and strategies for heat wave adaptation techniques (Tomlinson, Chapman et al. 2011).  In a study by Tomlinson, Chapman et al., the higher temperatures in the city center of Birmingham, UK indicated greater land development with high-rise buildings and structures when compared to the lower temperature in the sub-urban areas.

The seasonal and temporal changes in temperature were studied and observed by Janos Unge et al. in Hungary.  UHI measurements proved to be more useful to determine the urban-rural contrast statistical models in the unchanging weather conditions during the day (Klysik and Fortuniak 1999).  In a UHI study conducted in Poland, by Krzysztof Fortuniak et al., there was a greater contrast in temperature between urban and rural regions after sunset and during summer nights.  In another study by Janos Unge et al., the UHI values were highest in the city center and after sunset. Due to changes in the wind pattern, there were some irregularities seen in the

western part of the urban region of Poland as the cooler winds from the suburbs caused the urban temperature to drop (Unger, Sumeghy et al. 2003).

Thermal remote sensing has been widely used to measure surface temperatures. The land surface temperature influences the lower layers of the atmosphere which determines the climatic conditions of the urban and rural areas. Thermal remote sensors are different from the in situ measurements (Voogt and Oke 2003). The UHI measured using these sensors have wide spatial distribution with less temporal resolution where the information of atmospheric layers and surface heat radiation are required (Garcia-Cueto, Jauregui-Ostos et al. 2007). In a study by Garcia Cueto 2006, air temperatures recorded during each season of the year and the NOAA AVHRR images were used to study the characteristics of the urban area in the city of Mexico. The spatial analysis of extreme air temperatures (minimum and maximum) was performed. The image was classified in to zones based on the temperatures recorded. The UHI detected by satellites gave insights into the spatial distribution of vulnerable population affected by extreme heat (Johnson and Wilson 2009).

The traditional measurement of air temperature from weather stations is limited due to less spatial distribution of temperature monitoring locations; whereas, temperatures measurements using remotely sensed technologies, measure the land surface temperature (LST) over a wide urban area for Urban Heat Island studies (Zhang and Wang 2008). Surface Urban Heat Islands are studied using LST measurements using satellite remote sensing techniques. Various studies related to the climate modeling, global change, and heat-balance measurements utilize LST to determine the Earth's surface temperature (Yuan and Bauer 2007). The LST retrieved using Landsat TM images using the mono-window technique revealed better accuracy when compared with the near-surface air temperatures of the same region in Hong Kong (Liu and Zhang). Weng (2003) studied the spatial distribution of surface radiant temperatures

and its effect on UHI in Guangzhou, China. The UHI was investigated by analyzing transects drawn from the images. The areal extent of UHI changed according to the change of seasons(Weng 2003). The changes in land cover and urban development influenced the radiant temperatures as manifested in temperature differences between the urban and rural areas. The different land use and land cover types determine the surface temperatures and account to the differences in LST in urban and sub-urban areas (Lo, Quattrochi et al. 1997). The surface temperature is influenced by the radiant heat fluxes contributed by urbanization (Dousset and Gourmelon 2003).

Surface temperatures retrieved using Landsat TM data by calculating brightness, temperature and emissivity indicated regions of higher temperatures in the central business districts which have high land development when compared to the sub-urban regions (Huang, Shao et al. 2008).

LST pattern was studied in Beijing, China (Xiao, Weng et al. 2008) which indicated a positive correlation between built up density, buildings and population density; and a negative correlation between percentage of forest, farmland and water bodies. Although, analyzing and deriving the NDVI measurements are important for climate studies, the seasonal variations in vegetation influences the results of surface temperatures and hence, NDVI alone is not enough to measure the Surface Urban Heat Island quantitatively (Yuan and Bauer 2007). A study by F. Yuan, M.E. Bauer et al. (2007) indicates a strong linear relationship between LST and impervious surface and variable relationship between LST and NDVI. In the past, NDVI was used as an indicator to analyze the urban temperature changes. A study by (Lo, Quattrochi et al. 1997) examined the negative correlation between NDVI and irradiance of residential and vacant land cover types by studying the day and night airborne thermal infra-red images. (Gallo, Tarpley et al. 1995) studied the urban-rural temperature variations by examining

the NDVI which produced a statistically significant result that indicated less than 40% variation in air temperature differences between these two regions.

Many studies have incorporated socio-demographic variables to study the effects of extreme heat events on population. In a study by (Reid, O'Neill et al. 2009) the populations vulnerable to extreme heat were mapped for the United States by validating the health outcome data. This enabled identification of populations vulnerable to heat in geographic space and those that needed intervention in terms of medical care and attention. A study by (Harlan, Brazel et al. 2006), integrated the physical environmental characteristics with the socio-economic variables in a Phoenix neighborhood, to determine the most vulnerable populations with higher exposure to heat. A significant correlation was observed between high temperatures and open space or sparse vegetation. The downtown regions of all cities exhibited higher vulnerability when compared to the sub-urban regions (Reid, O'Neill et al. 2009).

The Extreme Heat Vulnerability Index (EHVI) was studied by (Stanforth) in 2011 to map the most vulnerable population to extreme heat with respect to the socio-demographic variables and examining the NDVI, NDBI and LST measurements for the Chicago area (1993). The population density, educational attainment and age resulted in best predictors of heat vulnerability.

Population statistics have been found to have little influence on the UHI. The use of population data alone in estimating UHI is not a preferred global method (Gallo and Owen 1999). Socio-demographic models utilizing LST to assess the vulnerable population in Philadelphia (2003) due to EHE has been studied by (Johnson, Wilson et al. 2009). This model suggested that the LST mean, LST maximum and the range is correlated with heat-related mortality rate. The use of LST data is important in predicting the risk associated with heat when compared to the models that use only socio-demographic variables to assess the heat related risks. In addition, by studying the

range of temperatures across the pixels within census tracts, the temperature values were used to compare the mortality and socio-demographic variables.  In another study by Johnson et al. (2013), the intensity of urban heat was measured using LST, where the UHI was much higher on heat event days than on normal summer days. The percentile ranks for each pixel were calculated by obtaining 16 cloud-free images for 2011 (Johnson et al. 2013, in press).

During the 1993 heat wave in Philadelphia, there were 118 heat related deaths reported by the medical examiner which is an underestimate according to Shen et al. 1998.  In 1995, the Philadelphia Hot Weather Health Watch/Warning System (PWWS) was developed in response to the health risks associated with extreme heat during the summer months of 1993 and 1994.  In addition, it served as an input for the National Weather Service to aid in implementation of emergency precautions and mitigation measures (Ebi, Teisberg et al. 2004).  According to the PWWS, heat warning was issued when the temperatures increased to 40.5 C for more than 3 hours a day on two consecutive days (Kalkstein, Jamason et al. 1996).  Further, in a study by Johnson, et al. (2009), the spatial association of heat-related deaths and the temperatures 308 K and 309 K were similar, which can prove to be environmental indicators to model Extreme Heat Events.  The likelihood of death increased in places where the mean and maximum LST were closer.  Moreover, the increase in the LST range suggested increased exposure to heat vulnerability (Johnson and Wilson 2009).

According to a study by Gaffen and Ross (1998), an extreme heat event day is classified based on the average air temperatures exceeding the 85th percentile of extreme heat stress events during the summertime, which is associated with mortality (Davis, Knappenberger et al. 2002).

The current study focused on measuring the extreme heat events quantitatively by using the percentile distribution of occurrences of high temperature regions.  This

research not only identifies the high-risk areas affected by extreme heat but also aids in taking precautionary measures, by introducing a comprehensive heat warning systems for future extreme heat events.

**DATA**

The study regions examined are Indianapolis and Philadelphia between the months of January and December of 2010 and 2011. These regions were susceptible to extreme heat events during the summer months.

Indianapolis, which is located in the Midwestern United States, has a total area of 368.2 square miles. It has four distinct seasons where the high temperature during summer is typically 90°F (32°C), and the low temperature during cold winters averages 28°F (-2°C). According to the National Weather Service temperature measurements, the highest recorded heat index in 2010 was 102.9°F on 13th August, and the corresponding maximum air temperature was 97°F (Table 1). The LST derived from Landsat imagery on this date was 308.901 K (96.35°F). In the year 2011, however, the highest recorded heat index was on 01 September with 101.2°F, and the corresponding maximum air temperature was 98.1°F (Table 2). The corresponding LST was 307.599 K (94.0°F). The higher temperature regions are mostly concentrated in the urban districts and the city center, whereas the lower temperatures are mostly in the sub-urban regions (Figure 7). Line graphs depicting the difference between the temperature measurements (in degree Fahrenheit) from the land surface recorded by Landsat TM 5 sensor, versus the ambient air from localized meteorological station is shown in the Figures 1 and 2 for the years 2010 and 2011, respectively.

Philadelphia is located in the Northeastern United States, and has an area of 142.6 square miles. It is characterized as having a humid sub-tropical climate; with hot and humid summers and mild to cold winters (according to the Koppen Climate Classification). It is reported as having occasional heat waves and high heat indices during summer months where the temperature reaches as high as 95°F (35°C). The average temperature in winter is 32.3°F (0.17°C). According to the temperatures recorded by the National Weather Service, the highest heat index in the year 2010 was

on 11 July with 89.3°F and the corresponding ambient maximum temperature was 91°F

(Table 3).  However, in the year 2011 the highest heat index recorded was on 30 July

and the corresponding ambient maximum temperature was 91°F. (Table 4).  The LST

measurement for 11 July 2010 was 310.733 K (99.65°F) and 330.207 K (134.70°F) on

30 July 2011 (Figure 8).  Line graphs depicting the difference between the temperature

measurements (in degree Fahrenheit) from the land surface recorded by Landsat TM 5

sensor, versus the ambient air from localized meteorological station is shown in the

Figures 3 and 4 for the years 2010 and 2011, respectively.

**METHODS**

The minimum and maximum digital numbers (DN) of the Landsat thermal images were converted to percentiles.  The minimum DN and the maximum DN of an image vary according to the thermal energy recorded at the sensor; at any given time (refer Tables 1 - 4).  The 90th, 95th, and 97th percentiles of the DN values were calculated in MS Excel.  The LST was derived only for the thermal band of the Landsat TM 5 images.  This yielded better and more accurate measurements compared to the LST derived using the stacked images of all the seven bands of Landsat TM 5.

The LST values corresponding to the percentiles were used to analyze the distribution of the regions with high temperatures during the extreme heat events.  The regions with greater than 90th percentile experienced extreme heat.

The areas having greater than 38 % cloud cover were not included in the calculation due to the potential erroneous results.  The larger extent of cloud cover is mainly seen in the cooler months of the year, during January, February, November, and December.  The unusual lower DN values during these months are attributed to the cloud cover.  Hence, the LSTs were also significantly lower.

**LST Conversion**

The Land Surface Temperatures were measured using Landsat 5 TM images with 120-metre spatial resolution which are resampled to 30 metre pixels during the image processing.  The LST was calculated using the ERDAS Imagine Modeler.  The LST conversion technique and equations have been originally studied and presented by Chander et al. (2007).  The application of constants for radiometric correction and calibration was further improved for Landsat TM 5 in 2007.  The thermal band in Landsat TM 5 is converted from at-sensor spectral radiance to at-sensor brightness temperatures using a calibration constant (Markham and Barker 1986).  The following equation

developed by National Aeronautics and Space Administration was used to convert the

original image to LST.

    a) Conversion of at-sensor spectral radiance

        The raw image with DN values is converted to spectral radiance.  The DN

        values range between 0 and 255.

$$L\lambda = \frac{Lmax\lambda - Lmin\lambda}{Qcalmax - Qcalmin} * (DN - Qcalmin) + Lmin\lambda$$

        Where,

        *$Lmax\lambda$ & $Lminx\lambda$ = Spectral at-sensor radiance (Band 6)*

        *$Qcalmax$ & $Qcalmin$ = Minimum and Maximum pixel values*

    b) Conversion of at-sensor spectral radiance to brightness temperatures

        (Planck's radiance equation)

$$T = \frac{K2}{\ln\left(\frac{K1}{L\lambda} + 1\right)}$$

        Where,

        *K1 and K2 = Thermal band calibration constants, 607.76 W/m²/sr¹/ɥm¹,*

        *1260.56 Kelvin*, respectively.

**Extreme Heat Events (EHE)**

        An extreme heat event refers to an extended period of high temperatures.

Extreme heat events were determined using the LST values.  The EHEs in the present

study were classified based on the LST values of the images obtained for 2010 and

2011 of Indianapolis and Philadelphia metropolitan regions.  The percentile ranks were

calculated based on the temperature values of the LST images corresponding to the DN

values.  The individual images were classified into "less than 90th", "90th", "95th", and

"97th" percentiles.  The LST was calculated only for the images with less than or equal to

38 % cloud cover (refer Figures 9 to 22). The percentiles represent thresholds for identifying days and regions affected by extreme heat.

**LST Composite Images**

The composite images for 2010 and 2011 were obtained by generating cell statistics for raster images (refer Figures 23 and 24). A composite output LST image was derived by calculating the average value of the inputs for each cell of the individual images, summed up to give a composite image. The output image consisted of the combined raster image. The combined cell statistics for raster images were derived for 2010 (Figure 23) and 2011 (Figure 24), to visually compare the extent of percentile distribution of heat with respect to land surfaces between the two years.

**RESULTS**

The surface temperatures obtained using the LST method and the ambient temperatures obtained from the meteorological stations showed a varied distribution. The corresponding maximum ambient air temperature values were plotted along with the maximum LST values for the purpose of visual comparison and to observe the trend (Figures 1 - 4).

In the Indianapolis region, LST was derived for thirteen Landsat TM 5 images obtained for the eight months of the year 2010 (*06 March, 09 May, 25 May, 10 June, 26 June, 12 July, 28 July, 13 August, 29 August, 30 September, 16 October, 01 November and 17 November*), with the cloud cover less than or equal to 38 %.  The highest mean LST for the year 2010 was on 25$^{th}$ May which measured 302.498 K (84.83°F).  The highest maximum LST for the year 2010 was on 25$^{th}$ May which measured 310.80 K (99.75°F).

For the year 2011, the LST was derived out of eleven Landsat TM 5 images obtained for the eight months (*04 January, 10 April, 13 June, 29 June, 15 July, 31 July, 16 August, 01 September, 17 September, 03 October, and 04 November*).  The highest mean LST for the year 2011 was on 29$^{th}$ June which measured 301.61 K (83.22°F).  The highest maximum LST for the year 2011 was on 29$^{th}$ June which measured 312.06 K (102.04°F).

For Philadelphia, there were 10 LST images derived for the year 2010 (*01 February, 21 March, 06 April, 25 June, 11 July, 28 August, 13 September, 31 October, and 02 December*), and 9 LST images for the year 2011 (*03 January, 08 March, 09 April, 11 May, 14 July, 30 July, 31 August, 16 September, 18 October*).  The highest mean LST for the year 2010 was 301.13 K (82.36°F) on 25$^{th}$ June, the highest maximum LST for the year 2010 was 312.61 K (103.02°F) on 25$^{th}$ June.  The highest mean LST for

the year 2011 was 303.98 K (87.50°F) on 30$^{th}$ July, and the highest maximum LST for the year 2011 was 330.21 K (134.70°F) on 30$^{th}$ July.

The spatial distribution of temperatures across the two cities depicted using percentiles provides a better comparison during different seasons. It is evident from the images that the summer months show a larger distribution of 95th and 97th percentiles, compared to the other months of the same year for both Indianapolis and Philadelphia (Figures 9 - 22). The area of percentiles calculated for the days with highest LST are represented in the pie-charts, along with the prior and subsequent months' LST values. This confirms our temperature recordings from the meteorological stations as well as those derived from the LST conversion (Figures 5 and 6).

Indianapolis:

In the 2010 images (Figures 9 - 13), the 95$^{th}$ and 97$^{th}$ percentiles covered the largest area for 25$^{th}$ May. The 90$^{th}$ percentile covered largest area for 29$^{th}$ August.

In the 2011 images (Figures 14 - 16), the 95$^{th}$ and 97$^{th}$ percentiles covered the largest area for 31$^{st}$ July, and 90$^{th}$ percentile covered largest area for 01$^{st}$ September. The percentile areas calculated for 29$^{th}$ June image were lesser than the percentiles areas of 31$^{st}$ July and 01 September, despite the highest LST value due to the fact that there was greater percentage of cloud cover (Tables 5 and 6).

Philadelphia:

In the year 2010, the area covered by 90$^{th}$ percentile was largest for 11 July. However, the 95$^{th}$ and 97$^{th}$ percentile area covered was the least (Figures 17 - 19). This is due to the cloud cover obscuring most parts of the region. The areas covered by 95th and 97th percentiles were largest for 25 June. In the year 2011, 97$^{th}$ percentile area was largest for 30$^{th}$ July (Tables 5 and 7).

**DISCUSSION**

The purpose of the study was to understand the distribution of extreme heat by analyzing and assessing its variations with respect to time, across Indianapolis and Philadelphia metropolitan regions for the years 2010 and 2011 using remotely sensed data.

Cloud cover across the cities limited the precise measurements of LST for a few of the images.  Hence, only the images with lesser than or equal to 38 % cloud cover were analyzed.  The results obtained are dependent on the remote sensing instruments and the atmospheric conditions during the image acquisition.

**Surface Temperature from Landsat TM 5**

The seven images of Indianapolis (10 June 2010, 13 August 2010, 29 August 2010, 16 October 2010, 29 June 2011, 31 July 2011, and 01 September 2011), and five images of Philadelphia (28 August 2010, 08 March 2011, 14 July 2011, 30 July 2011, and 31 August 2011) showed high spatial variations of LST due to clear weather conditions with less cloud cover during the summer season.  However, the regions with higher percentage of cloud cover show less spatial variations.  The spatial and temporal variations associated with different land cover types indicate the difference in surface emissivity.  The Land Surface Temperatures are higher in the urban areas than in the sub-urban areas.  This is due to the significant portion of the urban areas covered by asphalt, concrete or non-transpiring surfaces that radiate heat.  These include roof tops, roads, and pavements.  The spatial variations of heat vary seasonally and according to the moisture conditions.

**Percentile Calculation**

The analysis of Extreme Heat Events based on percentile calculation of the temperature values between the years, 2010 and 2011 for Indianapolis and Philadelphia revealed distinct spatial concentrations of 97th percentile during the summer months. The maps depicting the 97th percentile for 13th August and 29th August of 2010, and 29th June and 15th July of 2011 for Indianapolis, revealed a greater spatial variation compared to the other months.  Similarly, in Philadelphia, 25th June 2010, and 14th July 2011 and 30 July 2011 revealed a greater distribution of 97th percentile compared to the other months of respective years of the same region.  In contrast, less than 90th percentile and 90th percentile distribution across the months of 2010 and 2011 were more prominent between the months of March and June, and October to December. However, 95th percentile revealed a less spatial distribution compared to the 90th and 97th percentiles across the months of both the years of the two study regions.  The higher distribution of 97th percentile in the summer months is indicative of the higher urban development, and Urban Heat Island forms an important factor explaining such behavior.  The Extreme Heat Events observed in the summer months in relation to the Urban Heat Islands represents a positive trend between 2010 and 2011.

Further observations show that the highest maximum ambient temperature during the years 2010 and 2011, correspond to the days with the largest 90th percentile area.  The results, although inconclusive, show a trend in both the years.  Additional analysis of data for different years will be advantageous in understanding the percentile area for future studies.

**Limitations associated with LST measurements**

The Land Surface Temperature derived from Landsat TM 5 involves several assumptions.  The radiometric calibration for sensor correction used during conversion of Radiance to Temperature values has uncertainty of 5 % (Chander et al. 2010).  Apart from the sensor calculations and approximations, the atmospheric conditions with respect to the cloud cover, moisture content, aerosol, dust particles, etc., contribute to the differences in accurate measurement of LST.  The cloud cover has high albedo which reflects more sunlight compared to the land or water.  This influences the atmospheric air temperature and consequently interferes with the surface temperature measurements.

In addition, Landsat TM 5 has only one thermal band for obtaining the temperature values, hence, additional information with respect to the atmospheric profile involving atmospheric and radiometric corrections are necessary to retrieve accurate measurements (Qin, Karnieli et al. 2001).

**CONCLUSION**

The present study showed that measuring Extreme Heat Events using Landsat images is quantifiable and reliable.  The LST conversion of images is a direct method of obtaining land surface temperatures.  With the exclusion of socio-economic variables and census data, this method has proven to be adequate for representing the heat wave phenomenon spatially.  Furthermore, pre-processing the images with respect to elimination of cloud cover will yield better results.  Nonetheless, the percentile distribution corresponding to the LSTs has presented conclusive results and increased the scope of research.

**Further research and improvements**

Analysis of the Extreme Heat Events in Indianapolis and Philadelphia paves way for further research in measuring the extent of the spatial distribution of the percentiles, and its variation in time.  In order to produce more meaningful results, the images with cloud cover need to be masked and eliminated to render accurate derivations of LST. LST measurements using high spatial and high spectral resolution, available from instruments such as ASTER are also useful in determining the surface emissivity and albedo.  One of the drawbacks in using Landsat LST measurements is the coarser spatial variability due to less spatial resolution compared to other sensors.  This can be attributed to the fact that the thermal emissivity from urban surfaces is anisotropic.  In other words, the thermal properties of the urban surfaces differ at different angles of measurements.  The LST measurements using Landsat TM is restricted to the field of view of emissivity of the urban surfaces.  Newer models developed from ASTER data use multispectral scanners, where the bidirectional emissivity is measured, and the atmospheric corrections are applied (Voogt and Oke 2003).

Future study will incorporate the data related to the number of people hospitalized, suffered heat strokes, and heat-related deaths which will strengthen the

research leading to development of a comprehensive heat-warning system to bring about more awareness among the population, and to take needed precautionary measures during extreme heat conditions.

In addition, to further understand the spatial variability of percentiles, Moran's I autocorrelation will be worthwhile to analyze and evaluate the spatial pattern. It will be useful to determine the statistical significance of the occurrences of clusters with respect to temperatures and their variation over time.

| Month | Cloud cover | DN Values | | LST | | | | | Ambient Temp | | Heat Index |
|---|---|---|---|---|---|---|---|---|---|---|---|
| 2010 | % | Landsat TM 5 | | K | | | °F | | °F | | °F |
| | | Min | Max | Mean | Min | Max | Min | Max | Min | Max | |
| 6-Mar | 6.46 | 85 | 115 | 282.717 | 276.288 | 290.688 | 37.65 | 63.57 | 23 | 48 | |
| 9-May | 22.33 | 76 | 143 | 288.727 | 270.623 | 302.911 | 27.45 | 85.57 | 37 | 59 | |
| 25-May | 10.72 | 106 | 158 | 300.221 | 285.574 | 310.792 | 54.36 | 99.76 | 67 | 86 | 85.40 |
| 10-Jun | 0.42 | 106 | 156 | 293.341 | 290.828 | 308.456 | 63.82 | 95.55 | 61 | 85 | 83.00 |
| 26-Jun | 10.56 | 100 | 150 | 294.726 | 286.664 | 305.446 | 56.33 | 90.13 | 67 | 92 | 97.60 |
| 12-Jul | 35.84 | 87 | 145 | 292.66 | 282.639 | 302.82 | 49.08 | 85.41 | 69 | 87 | 87.10 |
| 28-Jul | 31.44 | 107 | 143 | 295.144 | 278.444 | 304.074 | 41.53 | 87.66 | 73 | 92 | 96.50 |
| **13-Aug** | **4.06** | **124** | **159** | **299.99** | **294.729** | **308.901** | **70.84** | **96.35** | **74** | **97** | **102.90** |
| 29-Aug | 0.28 | 134 | 156 | 300.703 | 300.131 | 309.025 | 80.57 | 96.58 | 71 | 96 | 94.80 |
| 30-Sep | 8.47 | 94 | 149 | 296.965 | 282.515 | 306.947 | 48.86 | 92.83 | 50 | 80 | |
| 16-Oct | 0.01 | 115 | 140 | 292.97 | 292.176 | 302.932 | 66.25 | 85.61 | 38 | 70 | |
| 1-Nov | 10.73 | 87 | 117 | 281.692 | 280.339 | 292.368 | 44.94 | 66.59 | 35 | 57 | |
| 17-Nov | 37.32 | 85 | 106 | 277.386 | 276.134 | 287.124 | 37.37 | 57.15 | 34 | 51 | |

Table 1.LST and Ambient air temperature values of Indianapolis for the year 2010

| Month | Cloud cover | DN Values | | LST | | | | | Ambient Temp | | Heat Index |
|---|---|---|---|---|---|---|---|---|---|---|---|
| 2011 | % | | | K | | | °F | | °F | | °F |
| | | Min | Max | Mean | Min | Max | Min | Max | Min | Max | |
| 10-Apr | 7.31 | 100 | 143 | 296.742 | 286.188 | 304.121 | 55.47 | 87.75 | 58 | 83 | 82.50 |
| 12-May | 46.08 | 32 | 160 | 289.805 | 259.965 | 308.464 | 8.27 | 95.57 | 68 | 84 | 82.20 |
| 13-Jun | 10.25 | 91 | 153 | 297 | 279.587 | 309.451 | 43.59 | 97.34 | 60 | 77 | |
| 29-Jun | 5.49 | 102 | 160 | 301.611 | 286.384 | 312.059 | 55.82 | 102.04 | 60 | 83 | 80.80 |
| 15-Jul | 7.77 | 73 | 161 | 301.135 | 294.252 | 311.77 | 69.98 | 101.52 | 67 | 89 | 86.10 |
| 31-Jul | 2.14 | 114 | 167 | 300.522 | 296.859 | 311.445 | 74.68 | 100.93 | 75 | 94 | 93.30 |
| 16-Aug | 9.5 | 103 | 161 | 296.644 | 285.17 | 310.29 | 53.64 | 98.85 | 60 | 83 | 81.60 |
| **1-Sep** | **0.19** | **135** | **155** | **300.63** | **299.202** | **307.599** | **78.89** | **94.01** | **73** | **99** | **101.20** |
| 17-Sep | 13.01 | 76 | 140 | 294.429 | 270.024 | 302.834 | 26.37 | 85.43 | 53 | 74 | |
| 3-Oct | 3.24 | 84 | 136 | 290.69 | 277.903 | 301.767 | 40.56 | 83.51 | 40 | 74 | |
| 4-Nov | 0.11 | 102 | 114 | 284.534 | 284.827 | 290.535 | 53.02 | 63.29 | 41 | 56 | |

Table 2.LST and Ambient air temperature values of Indianapolis for the year 2011

| Month | Cloud cover | DN Values | | LST | | | | | Ambient Temp | | Heat Index |
|---|---|---|---|---|---|---|---|---|---|---|---|
| 2010 | % | | | K | | | °F | | °F | | °F |
| | | Min | Max | Mean | Min | Max | Min | Max | Min | Max | |
| 1-Feb | 38.31 | 61 | 93 | 267.56 | 261.155 | 281.22 | 10.41 | 46.53 | 21 | 35 | |
| 21-Mar | 20.06 | 97 | 143 | 293.42 | 282.284 | 301.99 | 48.44 | 83.91 | 45 | 75 | |
| 6-Apr | 48.23 | 24 | 139 | 258.207 | 253.485 | 302.606 | -3.40 | 85.02 | 57 | 87 | 84.70 |
| 22-Apr | 13.92 | 99 | 142 | 293.871 | 284.068 | 304.195 | 51.65 | 87.88 | 48 | 72 | |
| **25-Jun** | **14.57** | **104** | **172** | **301.13** | **287.709** | **312.611** | **58.21** | **103.03** | **69** | **88** | **87.60** |
| **11-Jul** | **14.85** | **89** | **153** | **295.853** | **280.106** | **310.733** | **44.52** | **99.65** | **71** | **91** | **89.30** |
| 28-Aug | 0 | 124 | 164 | 300.7 | 295.195 | 310.602 | 71.68 | 99.41 | 57 | 84 | |
| 13-Sep | 22.42 | 102 | 144 | 270.167 | 280.266 | 299.807 | 44.81 | 79.98 | 57 | 80 | |
| 31-Oct | 24.24 | 67 | 121 | 280.12 | 265.991 | 294.265 | 19.11 | 70.01 | 39 | 60 | |
| 2-Dec | 26.89 | 73 | 105 | 276.856 | 265.827 | 287.527 | 18.82 | 57.88 | 30 | 41 | |

Table 3.LST and Ambient air temperature values of Philadelphia for the year 2010

| Month | Cloud cover | DN Values | | LST | | | | | Ambient Temp | | Heat Index |
|---|---|---|---|---|---|---|---|---|---|---|---|
| 2011 | % | | | | K | | °F | | °F | | °F |
| | | Min | Max | Mean | Min | Max | Min | Max | Min | Max | |
| 3-Jan | 1.21 | 78 | 95 | 272.86 | 240.549 | 287.587 | -26.68 | 57.99 | 25 | 36 | |
| 8-Mar | 0.03 | 86 | 119 | 283.09 | 275.377 | 309.736 | 36.01 | 97.85 | 27 | 48 | |
| 9-Apr | 18.22 | 69 | 135 | 287.4 | 264.918 | 323.94 | 17.18 | 123.42 | 37 | 59 | |
| 11-May | 32.74 | 95 | 158 | 291.661 | 280.407 | 362.92 | 45.06 | 193.59 | 46 | 72 | |
| 14-Jul | 0.25 | 100 | 169 | 302.022 | 292.187 | 327.177 | 66.27 | 129.25 | 64 | 86 | |
| **30-Jul** | **0.14** | **135** | **171** | **303.978** | **294.486** | **330.207** | **70.40** | **134.70** | **73** | **91** | **90.60** |
| 31-Aug | 0.29 | 114 | 166 | 299.273 | 288.121 | 328.023 | 58.95 | 130.77 | 60 | 84 | 82.00 |
| 16-Sep | 10.65 | 103 | 145 | 291.223 | 279.787 | 318.97 | 43.95 | 114.48 | 46 | 54 | |
| 18-Oct | 19.16 | 103 | 136 | 288.447 | 262.385 | 314.63 | 12.62 | 106.66 | 46 | 71 | |

Table 4.LST and Ambient air temperature values of Philadelphia for the year 2011

| City | Date/Year | Mean LST | Maximum LST |
|---|---|---|---|
| Indianapolis | 25-May-2010 | 302.498 K (84.83 °F) | 310.80 K (99.75 °F) |
| Indianapolis | 29-Jun-2011 | 301.61 K (83.23 °F) | 312.06 K (102.04 °F) |
| | | | |
| Philadelphia | 25-Jun-2010 | 301.13 K (82.36 °F) | 312.61 K (103.02 °F) |
| Philadelphia | 30-Jul-2011 | 303.98 K (87.50 °F) | 330.21 K (134.70 °F) |

Table 5.Highest LST days in Indianapolis and Philadelphia for 2010 and 2011

| Year | Cloud cover | Percentile (Sq. Miles) | | | LST | | Air Temperature (°F) |
|---|---|---|---|---|---|---|---|
| 2010 | % | 90th | 95th | 97th | K | °F | |
| 25-May | 10.72 | 2652.764 | 5.135 | 4.295 | 310.80 | 99.75 | 86 |
| 28-Jul | 31.44 | 25.880 | 0.013 | 0.009 | 304.07 | 87.66 | 92 |
| 13-Aug | 4.06 | 246.404 | 3.431 | 2.722 | 308.90 | 96.35 | 97 |
| 29-Aug | 0.28 | 311.097 | 0.726 | 0.472 | 309.03 | 96.58 | 96 |
| | | | | | | | |
| 2011 | | 90th | 95th | 97th | K | °F | |
| 29-Jun | 5.49 | 275.497 | 8.073 | 6.619 | 312.06 | 82.42 | 83 |
| 15-Jul | 7.77 | 280.831 | 7.840 | 5.864 | 311.77 | 101.52 | 89 |
| 31-Jul | 2.14 | 255.005 | 8.468 | 6.764 | 311.45 | 100.93 | 94 |
| 16-Aug | 9.5 | 149.036 | 2.880 | 2.420 | 310.29 | 98.85 | 83 |
| 1-Sep | 0.19 | 332.221 | 0.318 | 0.210 | 307.60 | 94.01 | 99 |

Table 6.Percentile area for the summer months of 2010 and 2011 for Indianapolis

| Year | Cloud cover | Percentile (Sq. Miles) | | | LST | | Air Temperature (°F) |
|---|---|---|---|---|---|---|---|
| **2010** | **%** | **90th** | **95th** | **97th** | **K** | **°F** | |
| 28-Aug | 0.00 | 111.490 | 0.451 | 0.144 | 310.60 | 99.41 | 84 |
| 25-Jun | 14.57 | 95.279 | 7.540 | 2.736 | 312.61 | 103.03 | 88 |
| 11-Jul | 14.85 | 52.366 | 0.007 | 0.004 | 310.73 | 99.65 | 91 |
| | | | | | | | |
| **2011** | | **90th** | **95th** | **97th** | **K** | **°F** | |
| 14-Jul | 0.25 | 115.720 | 2.239 | 0.510 | 327.18 | 129.25 | 86 |
| 30-Jul | 0.14 | 112.723 | 10.465 | 3.710 | 330.21 | 134.70 | 91 |
| 31-Aug | 0.29 | 96.312 | 0.132 | 0.063 | 328.02 | 130.77 | 84 |

Table 7.Percentile area for the summer months of 2010 and 2011 for Philadelphia

Figure 1.A line graph showing LST versus air temperature measurements for the year

2010 in Indianapolis



Figure 2.A line graph showing LST versus air temperature measurements for the year

2011 in Indianapolis
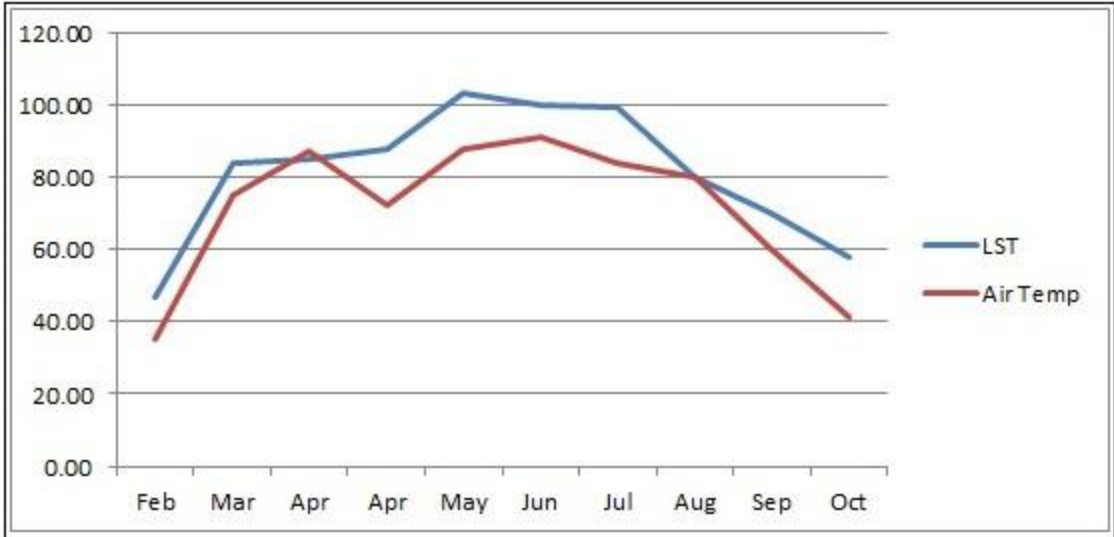
Figure 3.A line graph showing LST versus air temperature measurements for the year

2010 in Philadelphia
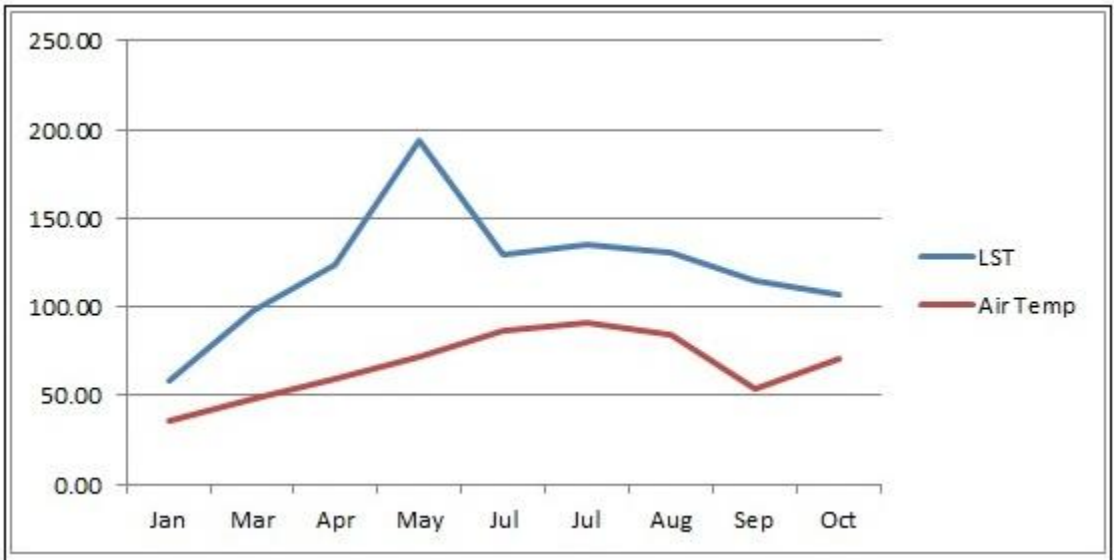


Figure 4.A line graph showing LST versus air temperature measurements for the year

2011 in Philadelphia
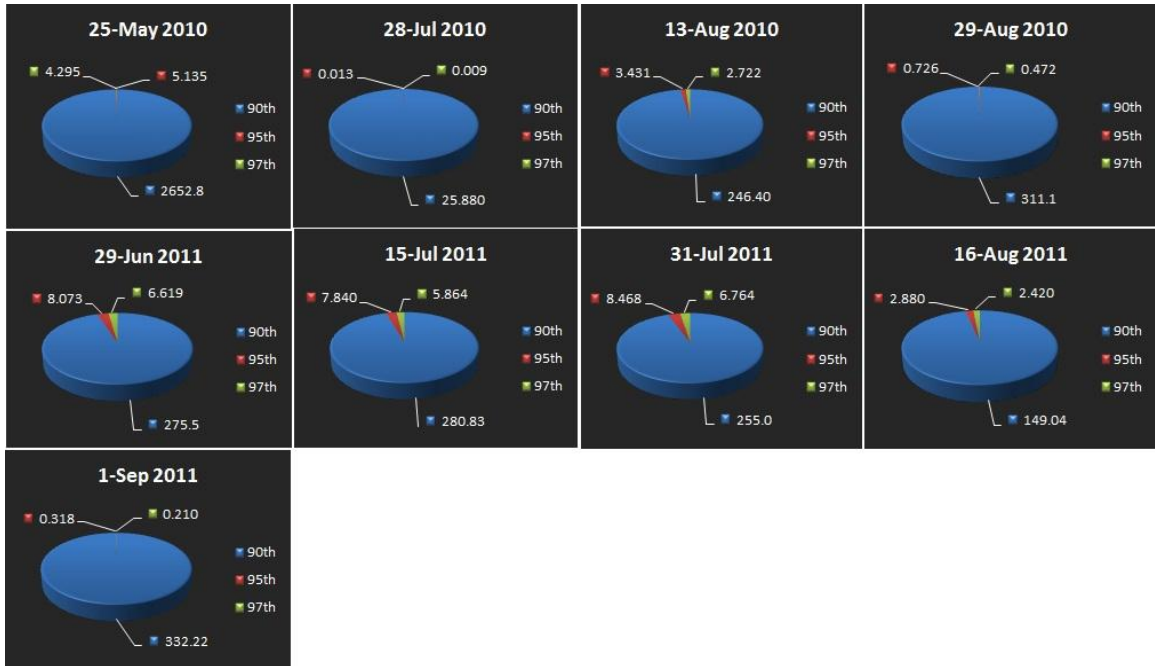
Figure 5 Pie-charts showing area of percentile distribution of heat

for the years 2010 and 2011 in Indianapolis
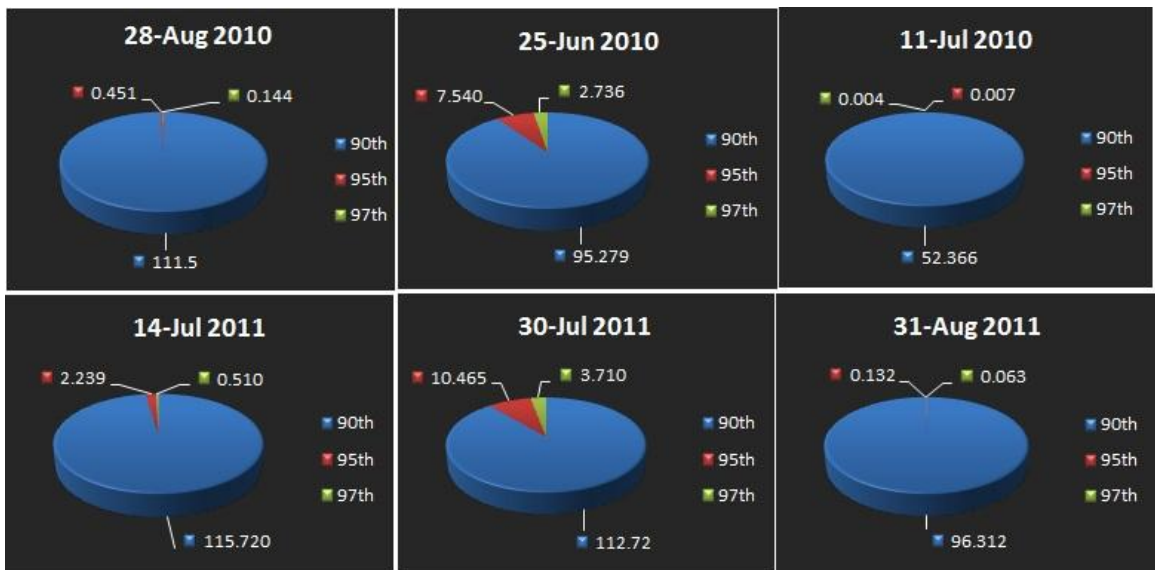


Figure 6.Pie-charts showing area of percentile distribution of heat

for the years 2010 and 2011 in Philadelphia
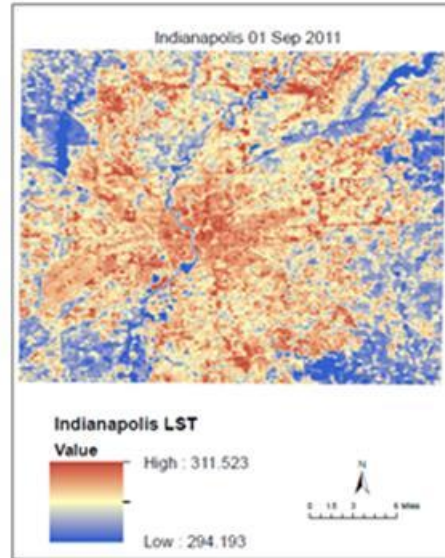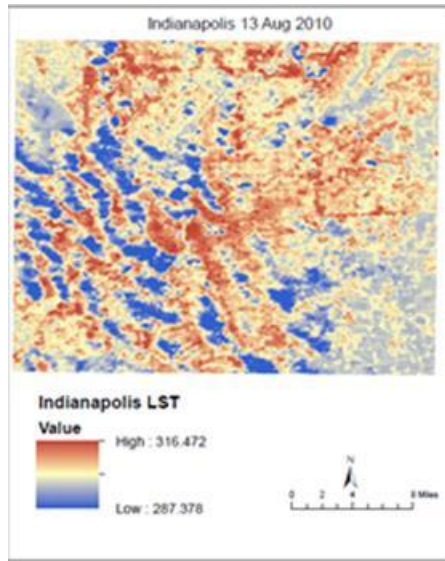
Figure 7.Maps showing highest air temperature recorded for the years 2010 and 2011 in
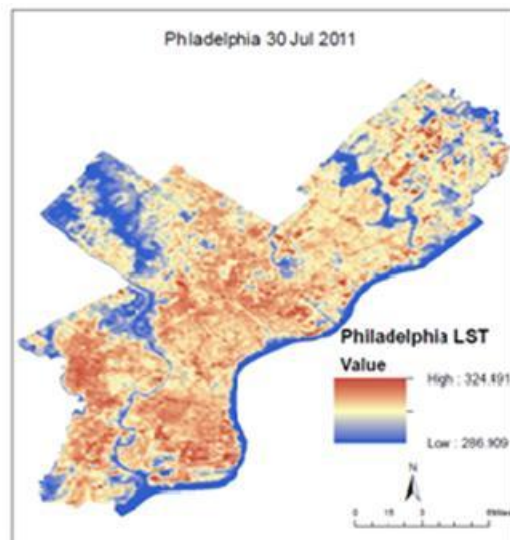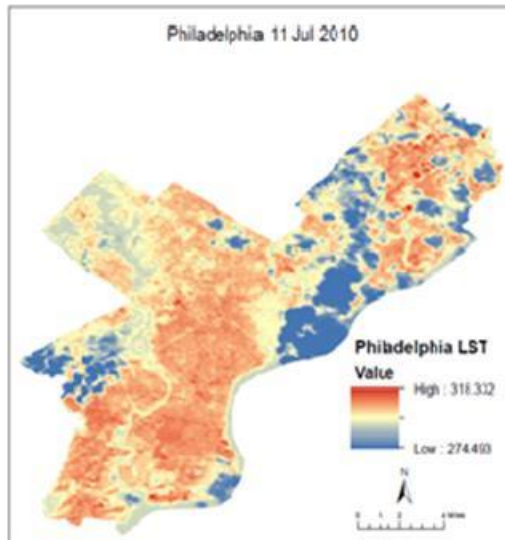
Indianapolis



Figure 8.Maps showing highest air temperature recorded for the years 2010 and 2011 in

Philadelphia
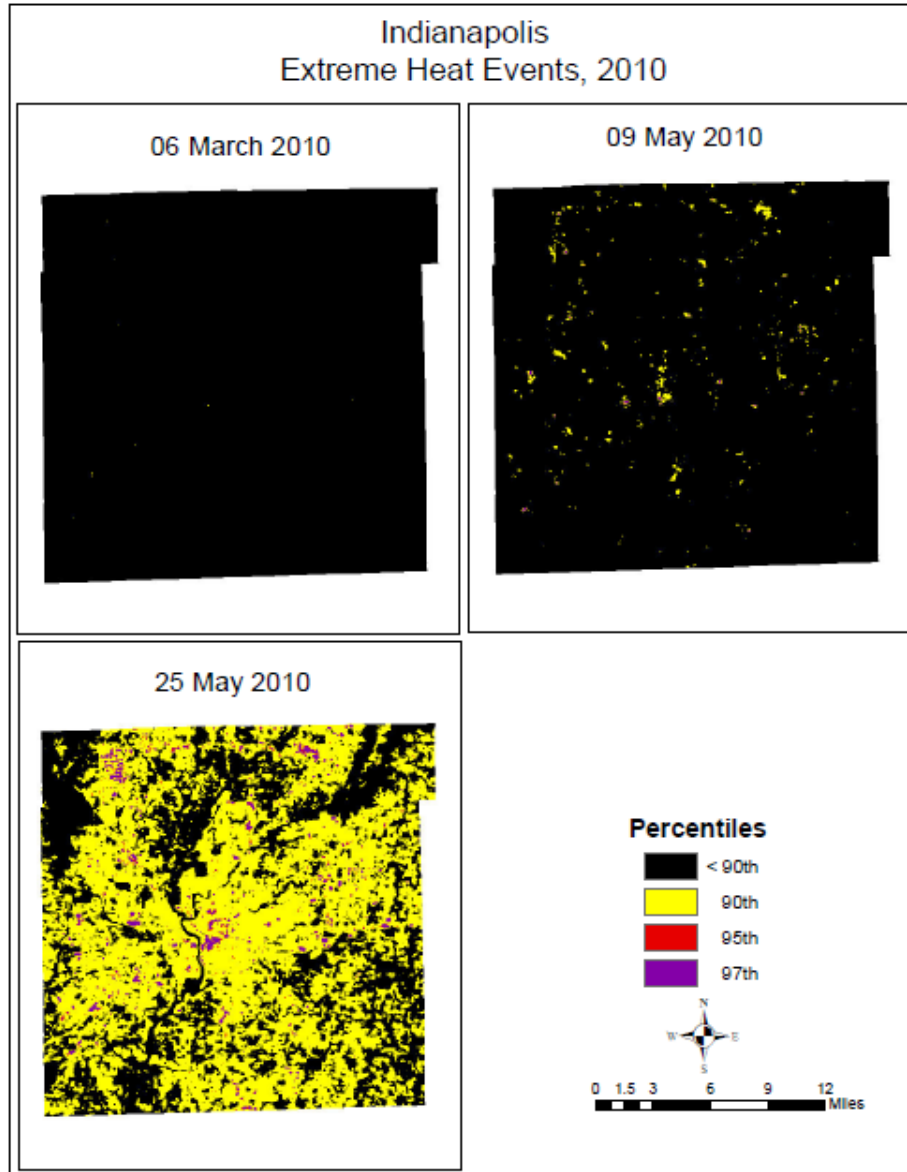
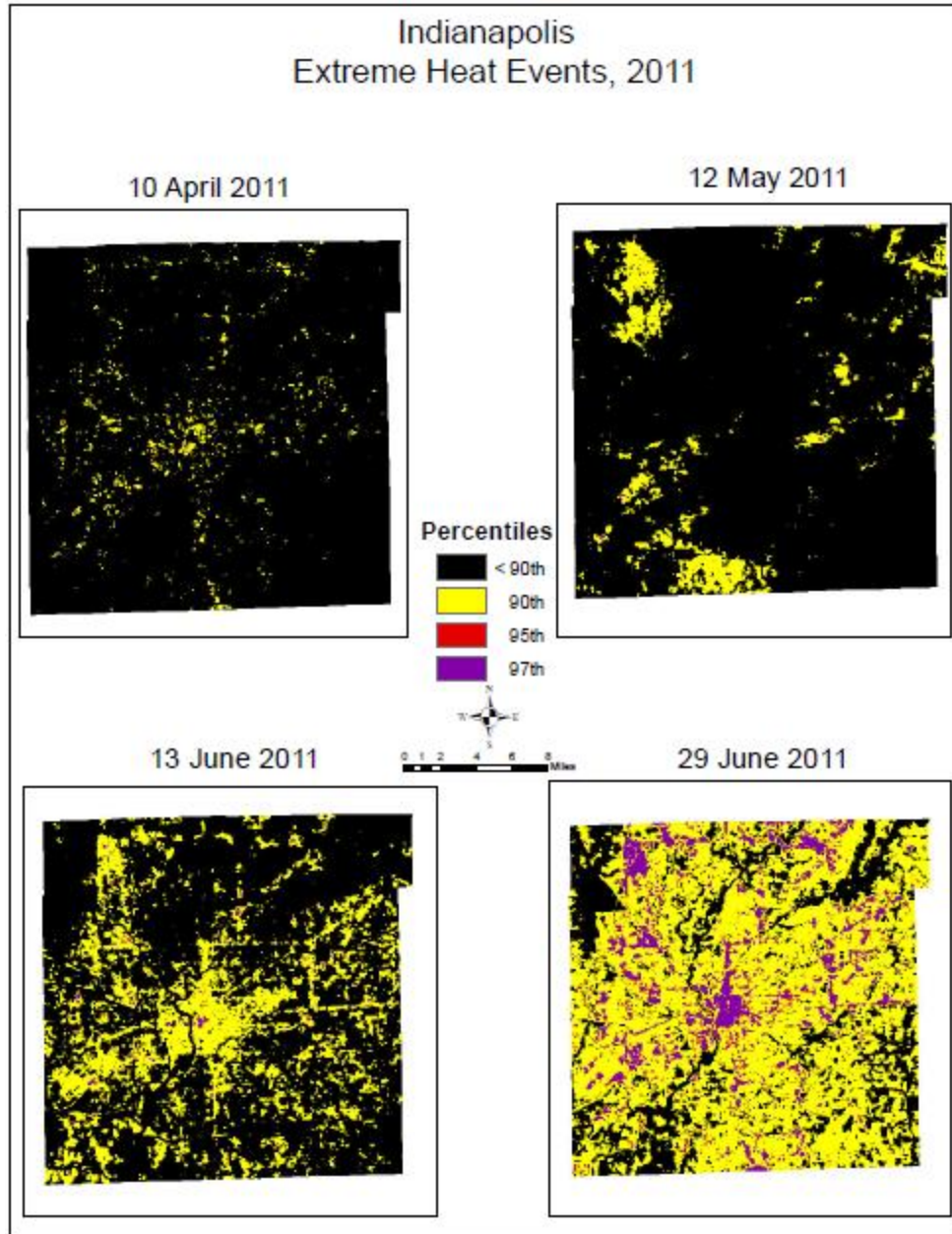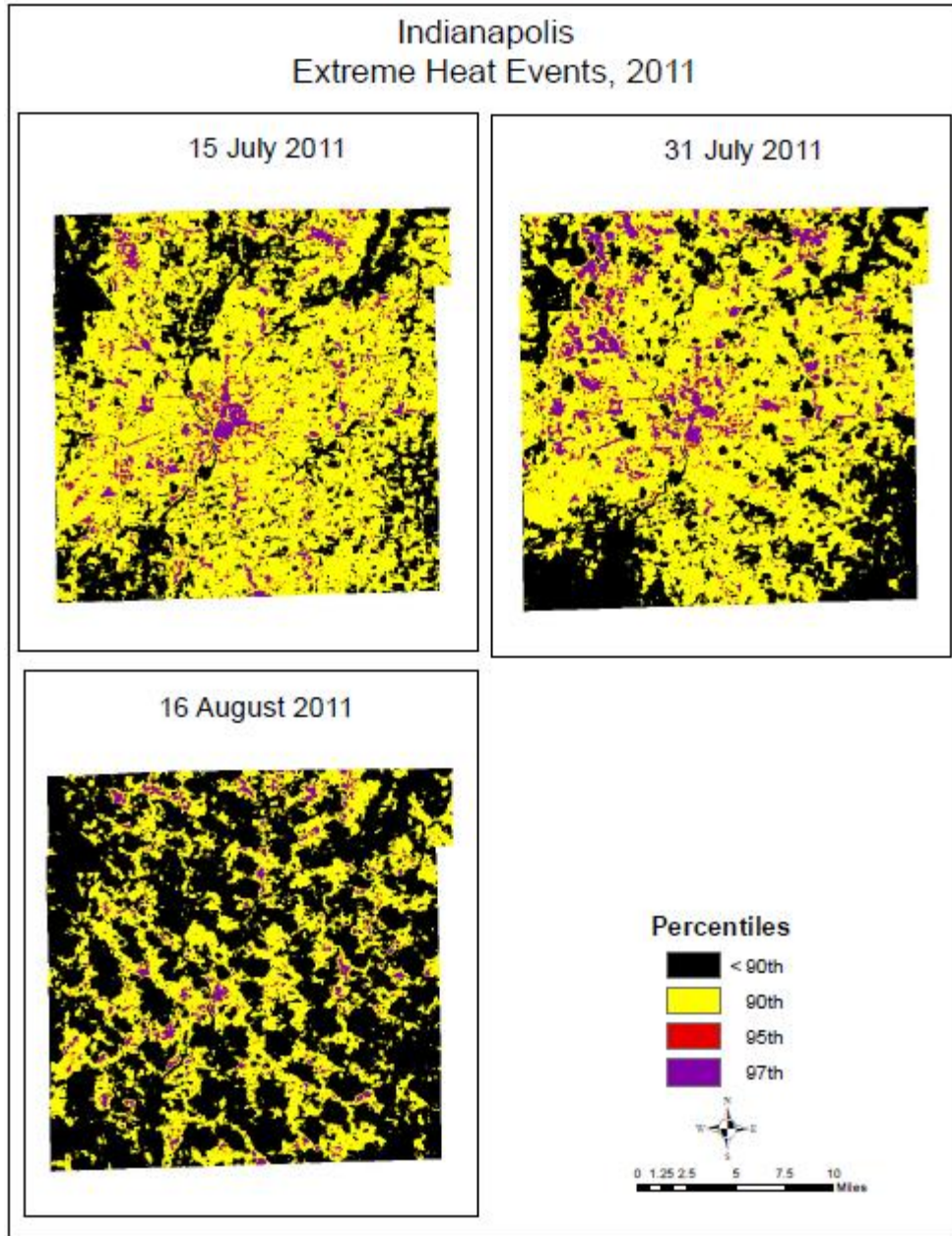Figure 9.Map showing percentile distribution of heat in Indianapolis
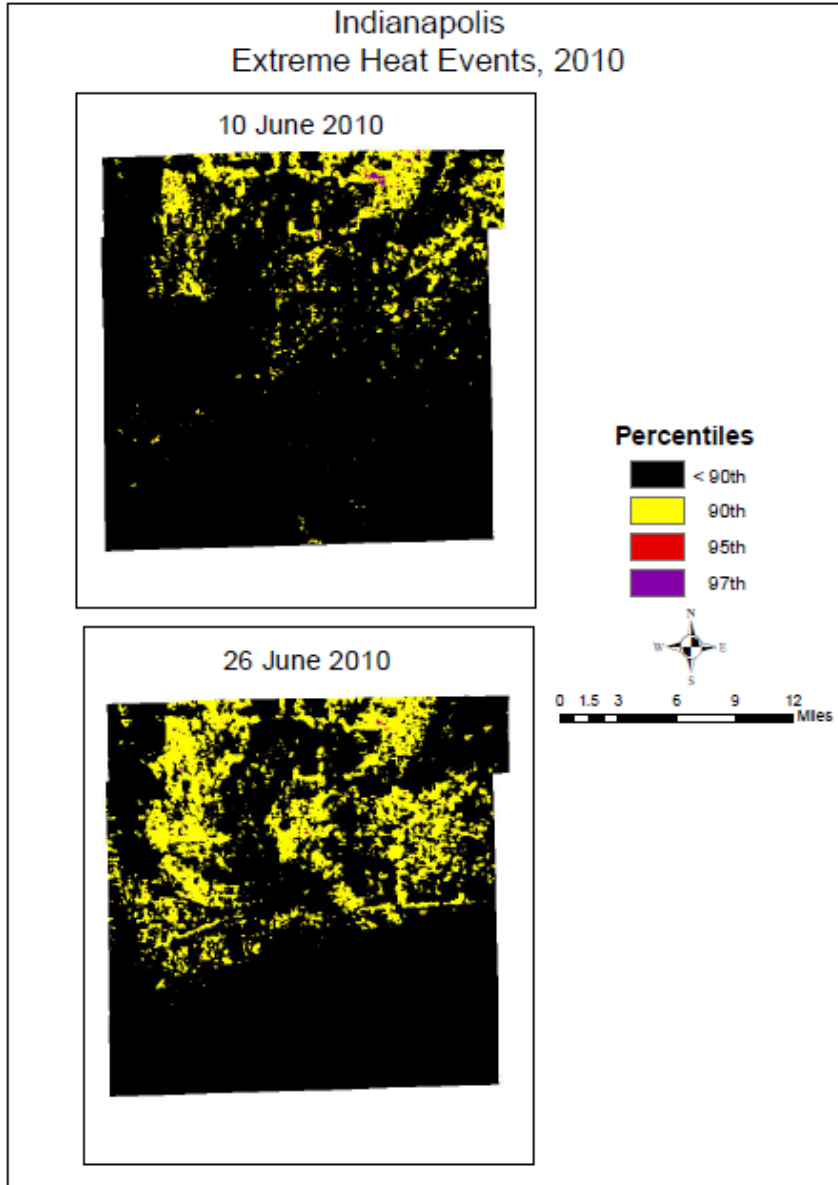
Figure 10.Map showing percentile distribution of heat in Indianapolis
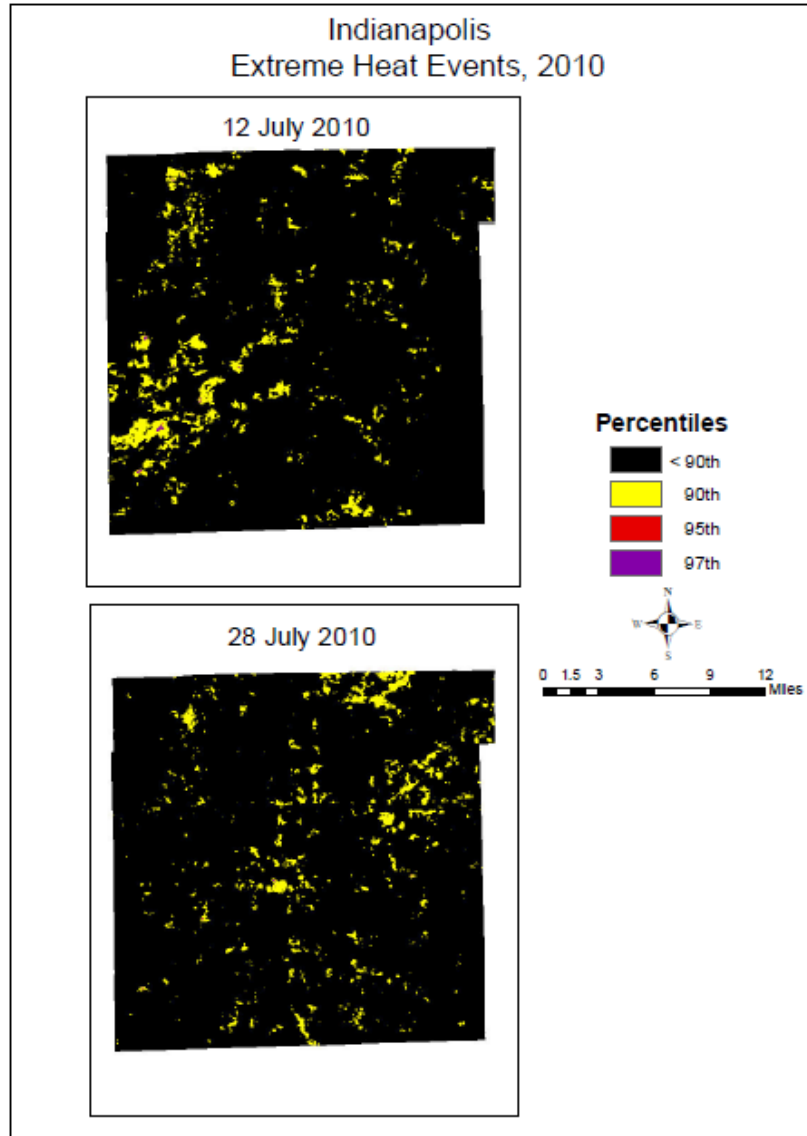
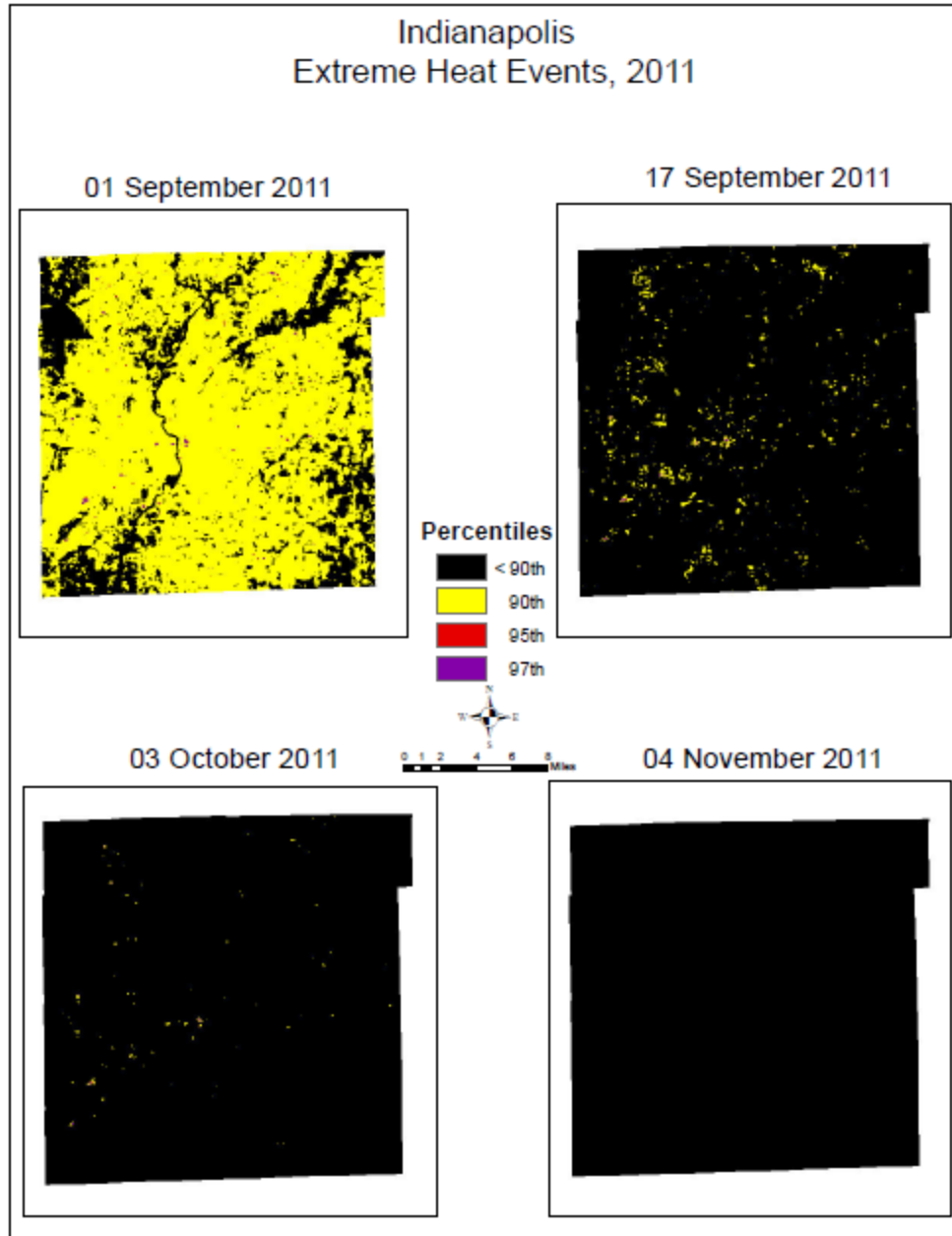Figure 11.Map showing percentile distribution of heat in Indianapolis
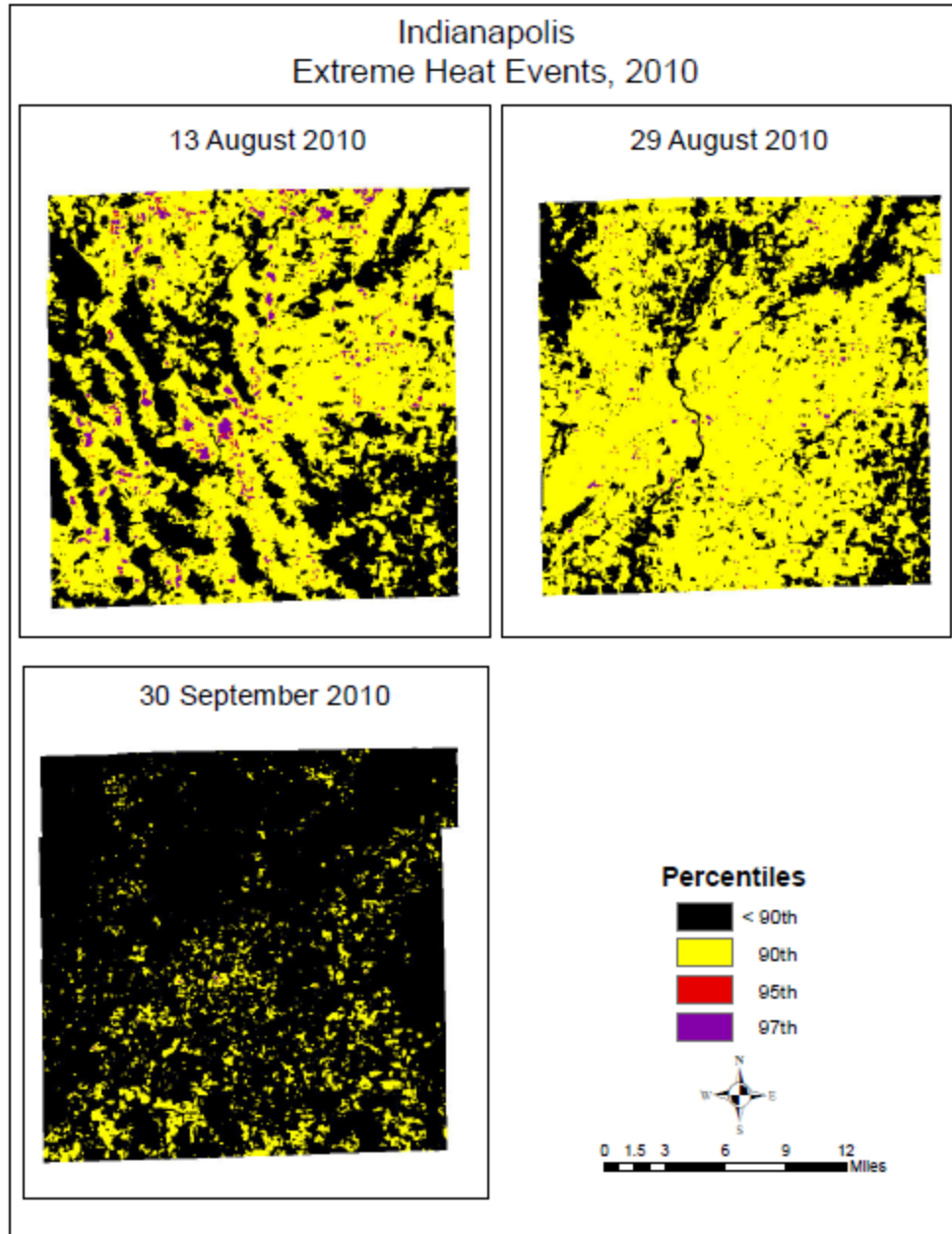
Figure 12.Map showing percentile distribution of heat in Indianapolis
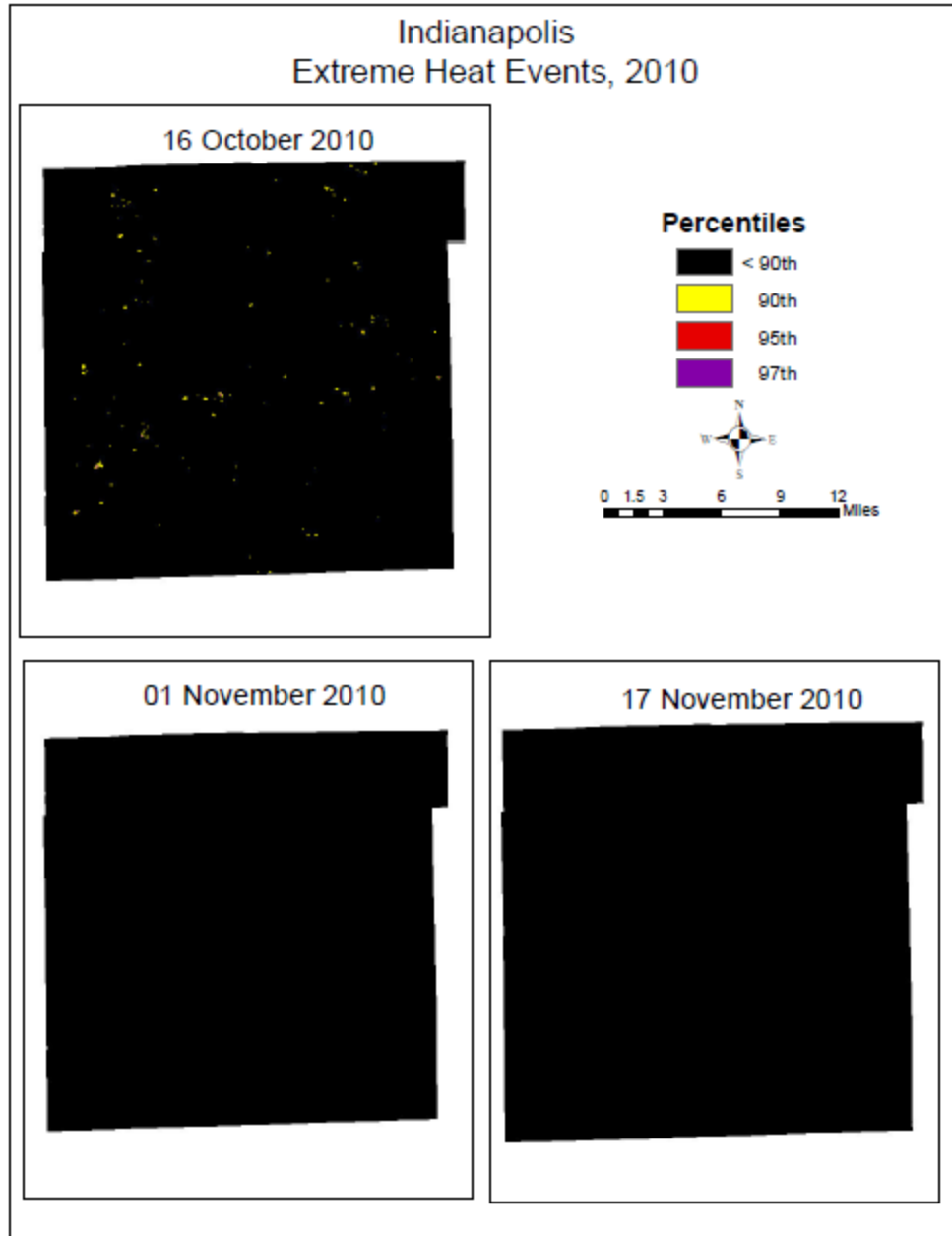
Figure 13.Map showing percentile distribution of heat in Indianapolis

Figure 14.Map showing percentile distribution of heat in Indianapolis

Figure 15.Map showing percentile distribution of heat in Indianapolis

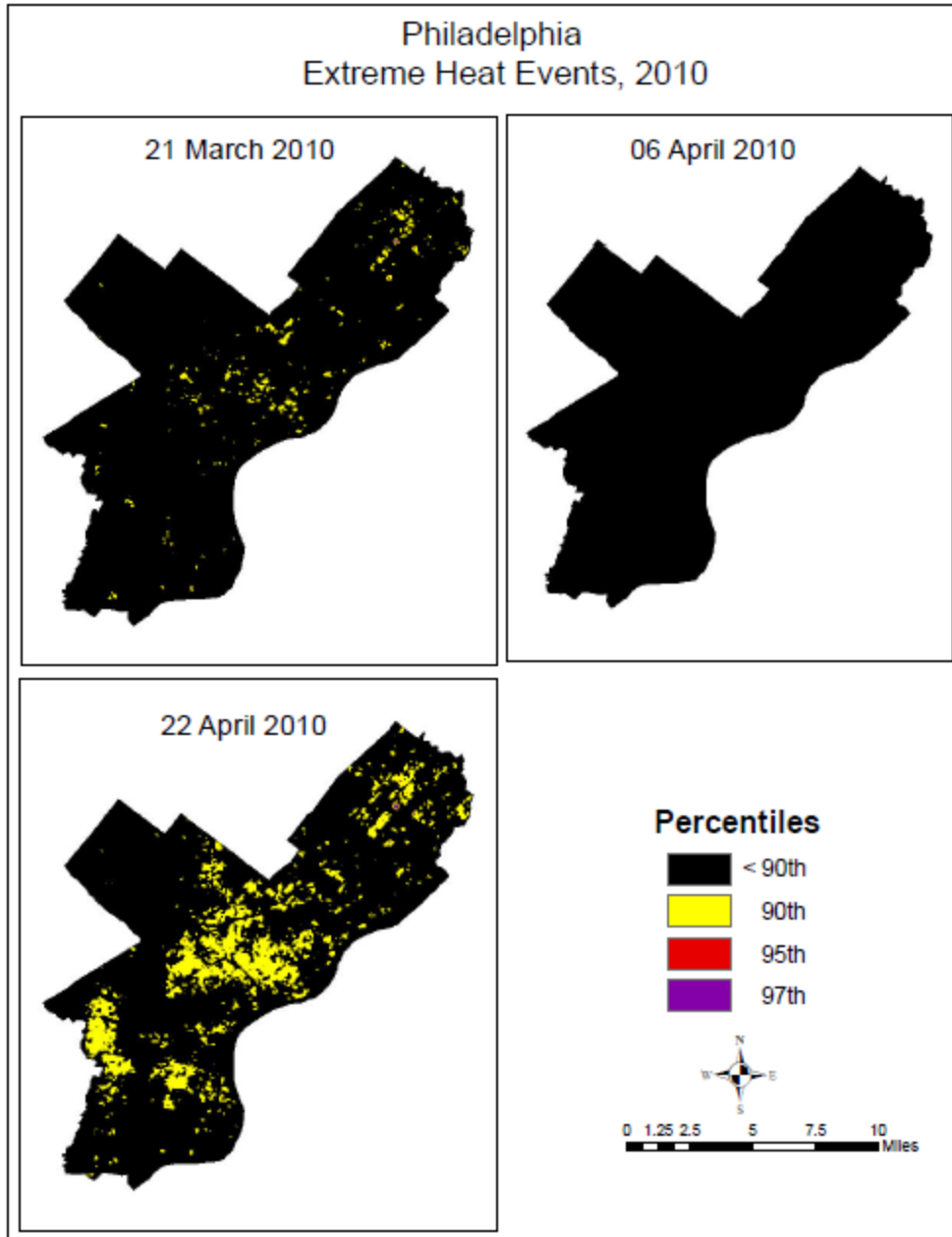Figure 16.Map showing percentile distribution of heat in Indianapolis

Figure 17.Map showing percentile distribution of heat in Philadelphia
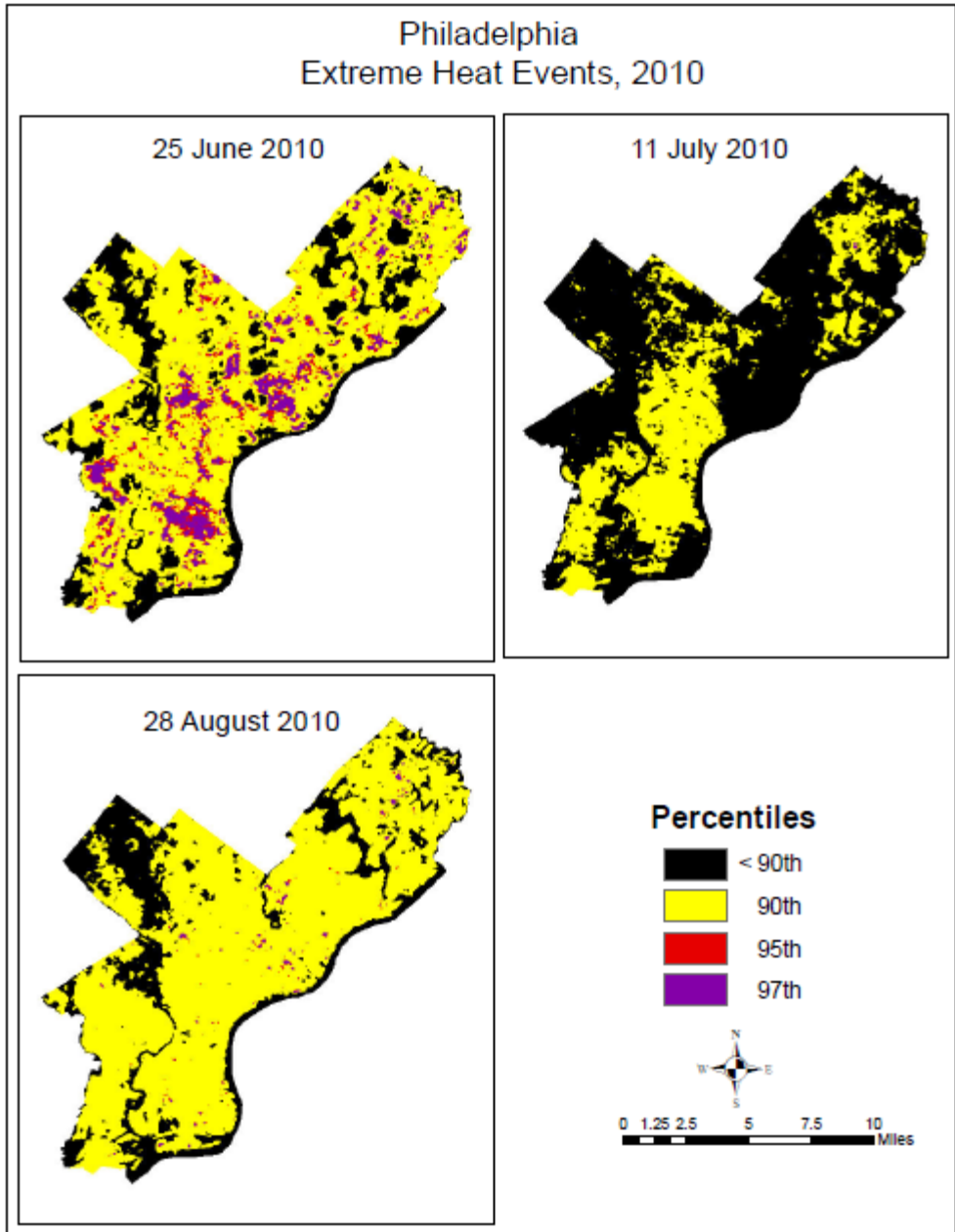
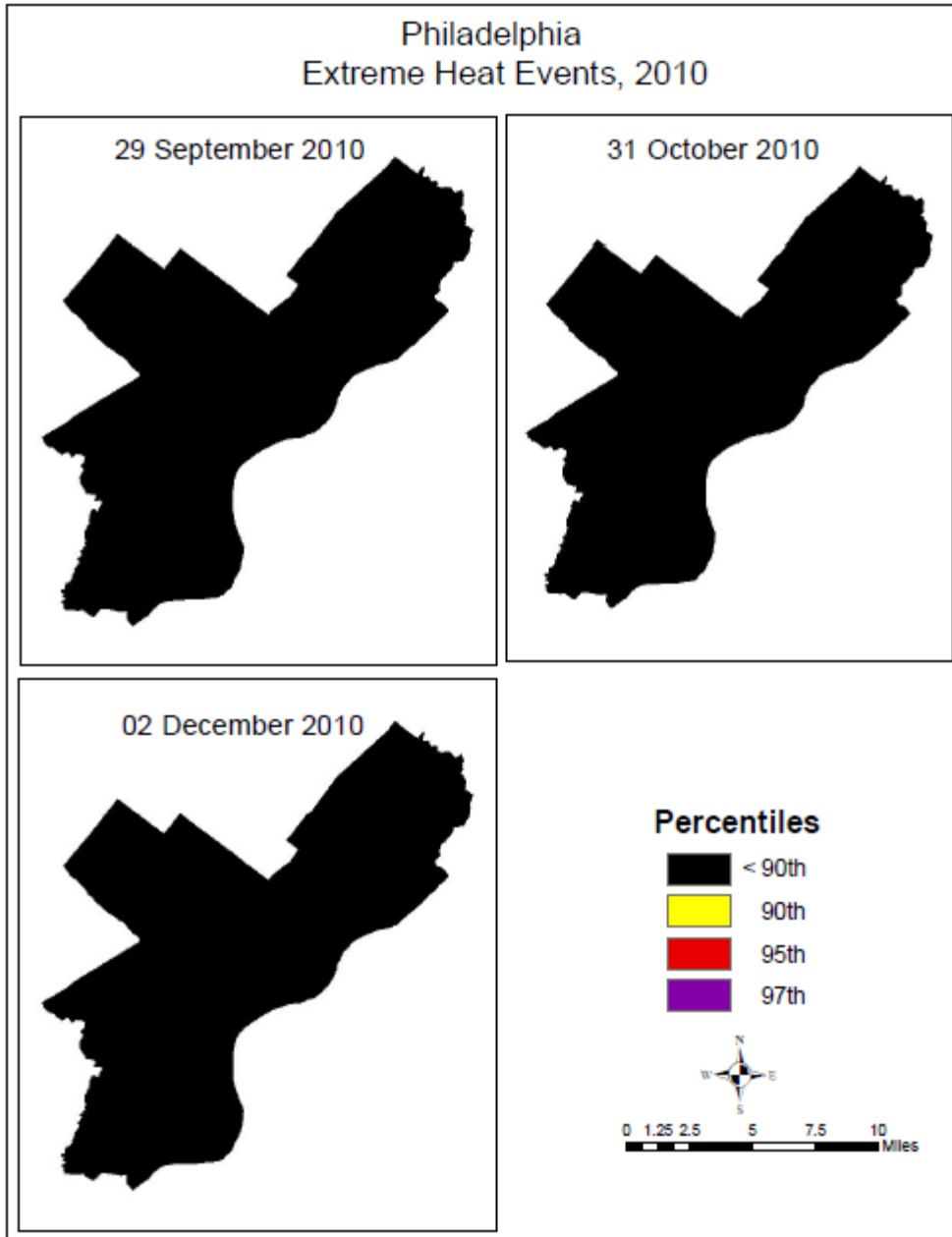Figure 18.Map showing percentile distribution of heat in Philadelphia

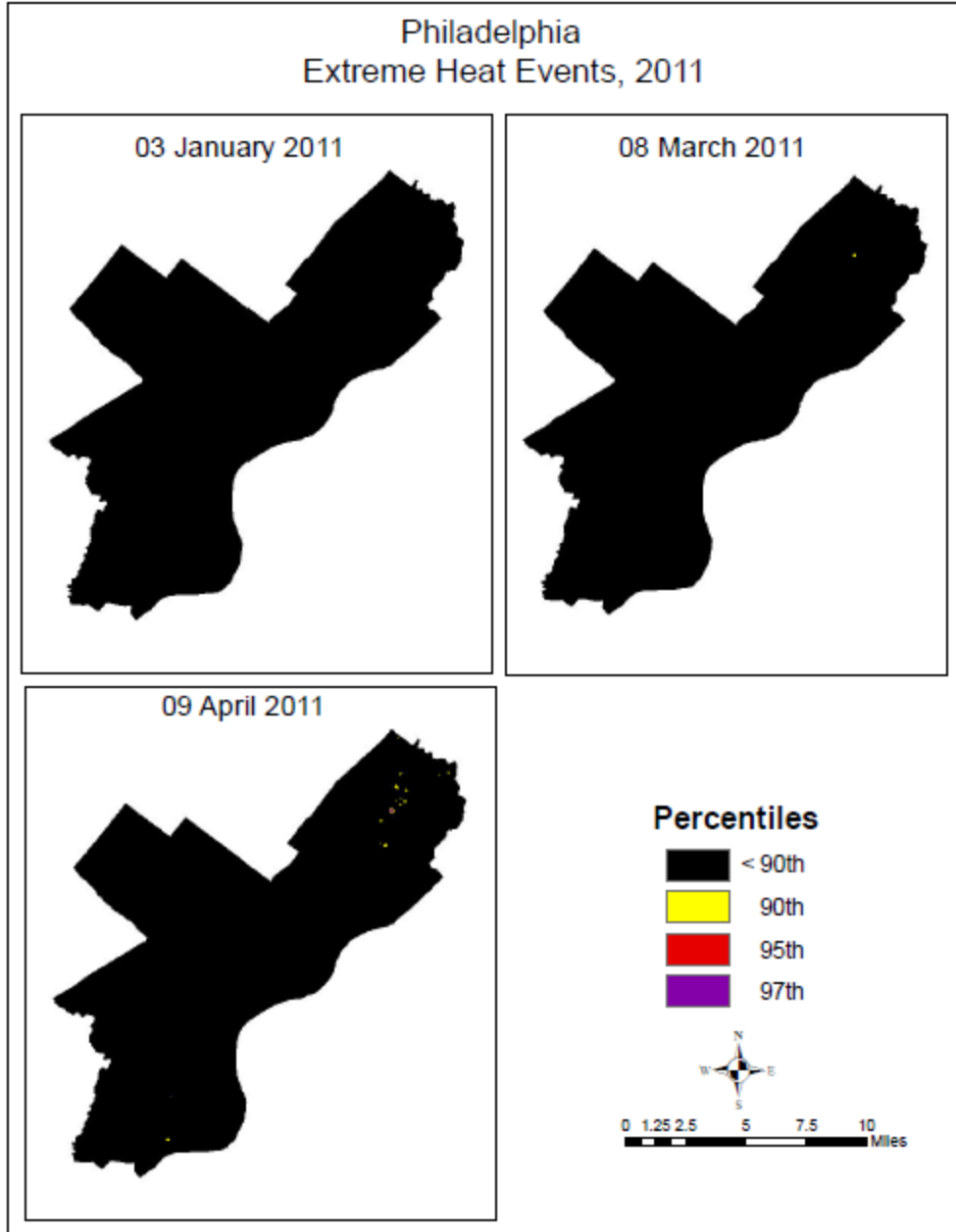Figure 19.Map showing percentile distribution of heat in Philadelphia

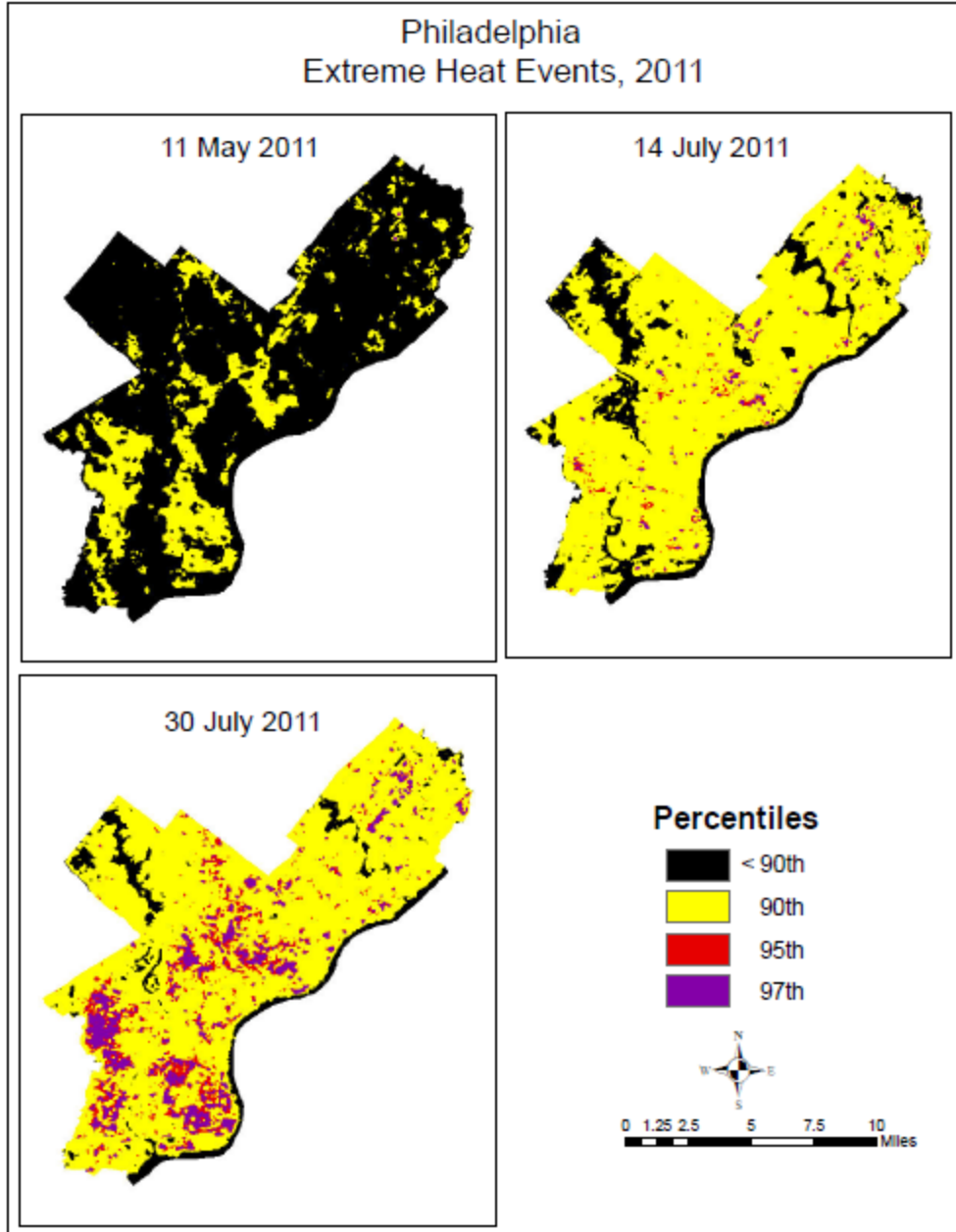Figure 20.Map showing percentile distribution of heat in Philadelphia

Figure 21.Map showing percentile distribution of heat in Philadelphia
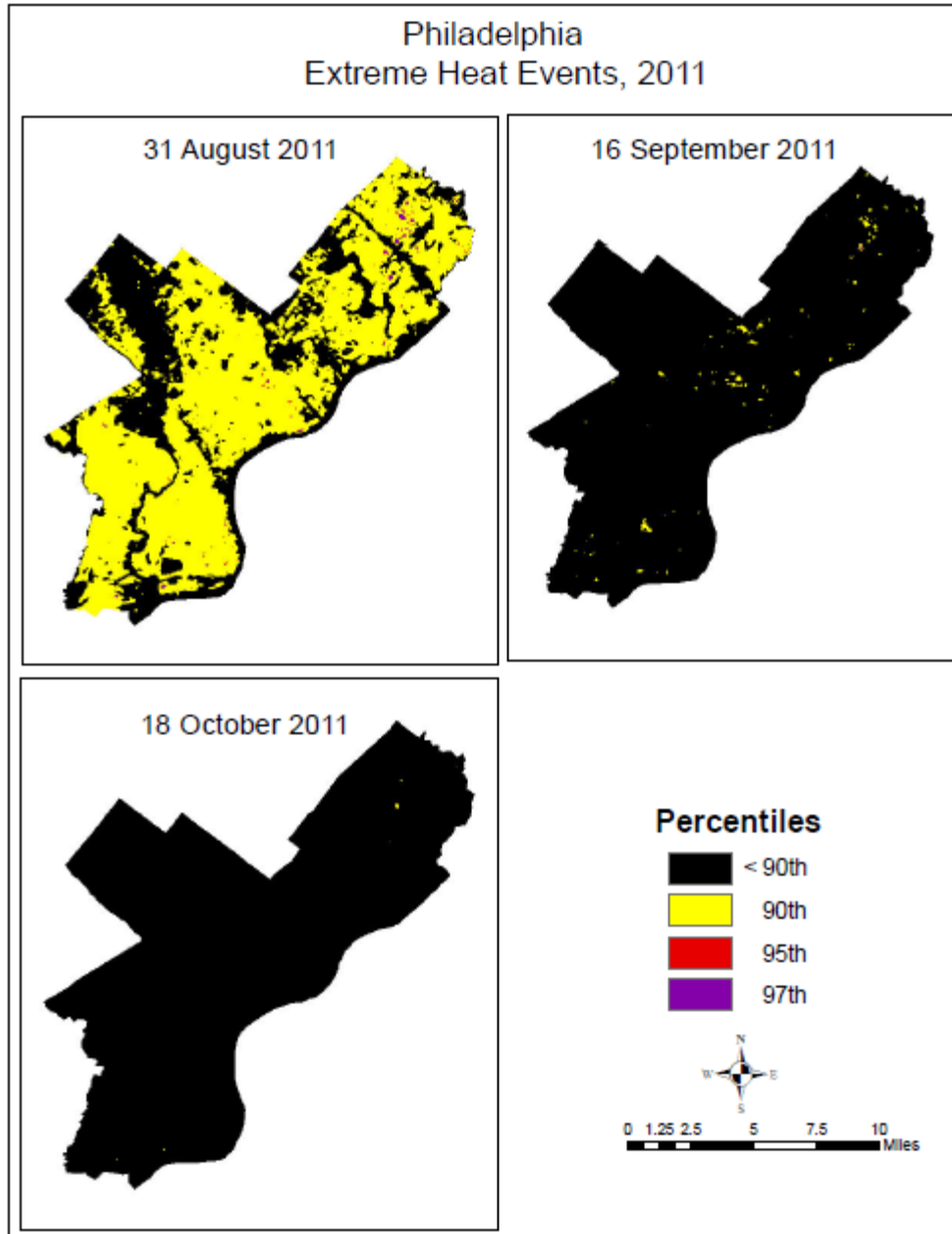
Figure 22.Map showing percentile distribution of heat in Philadelphia
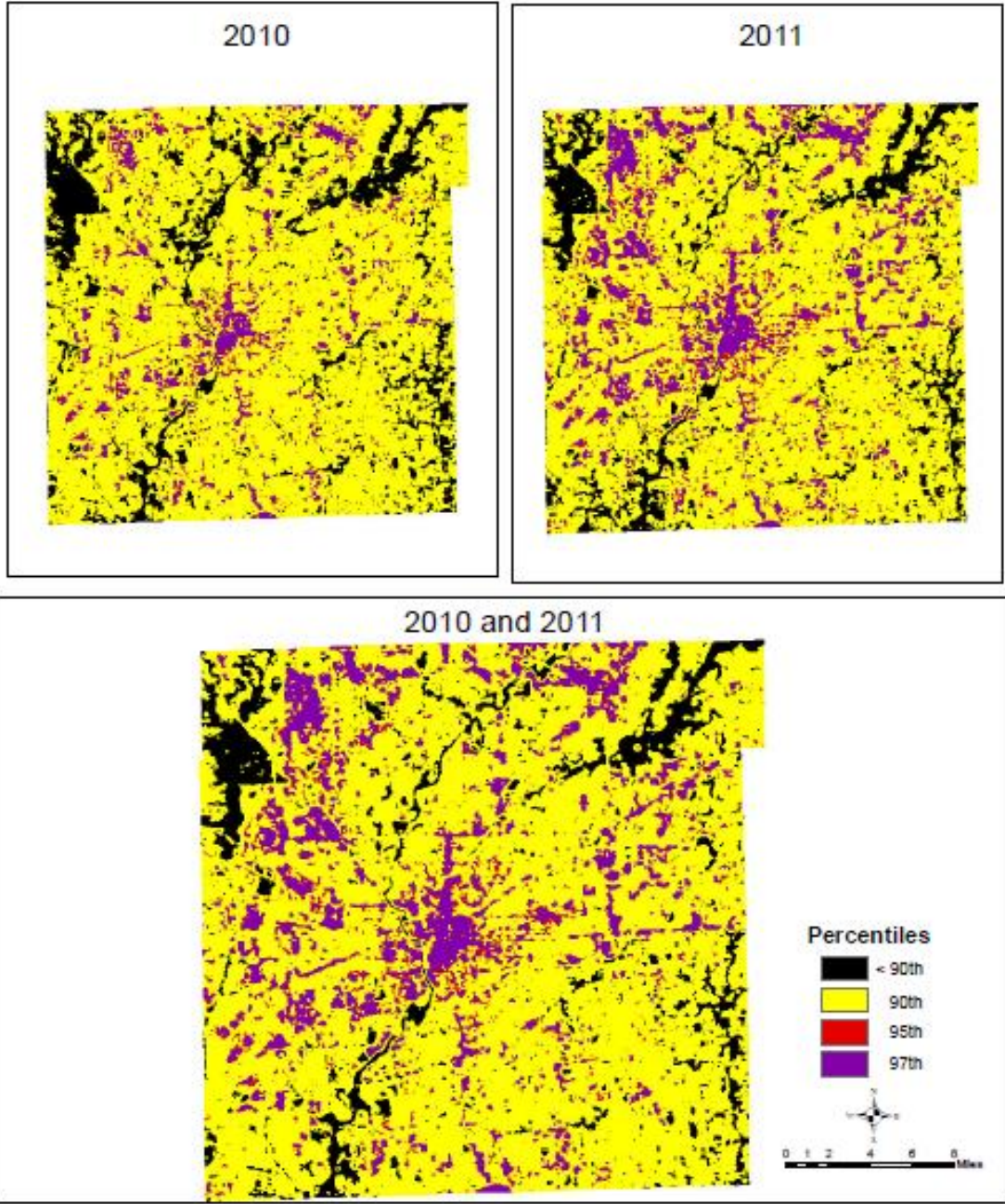
# Indianapolis
## Extreme Heat Events



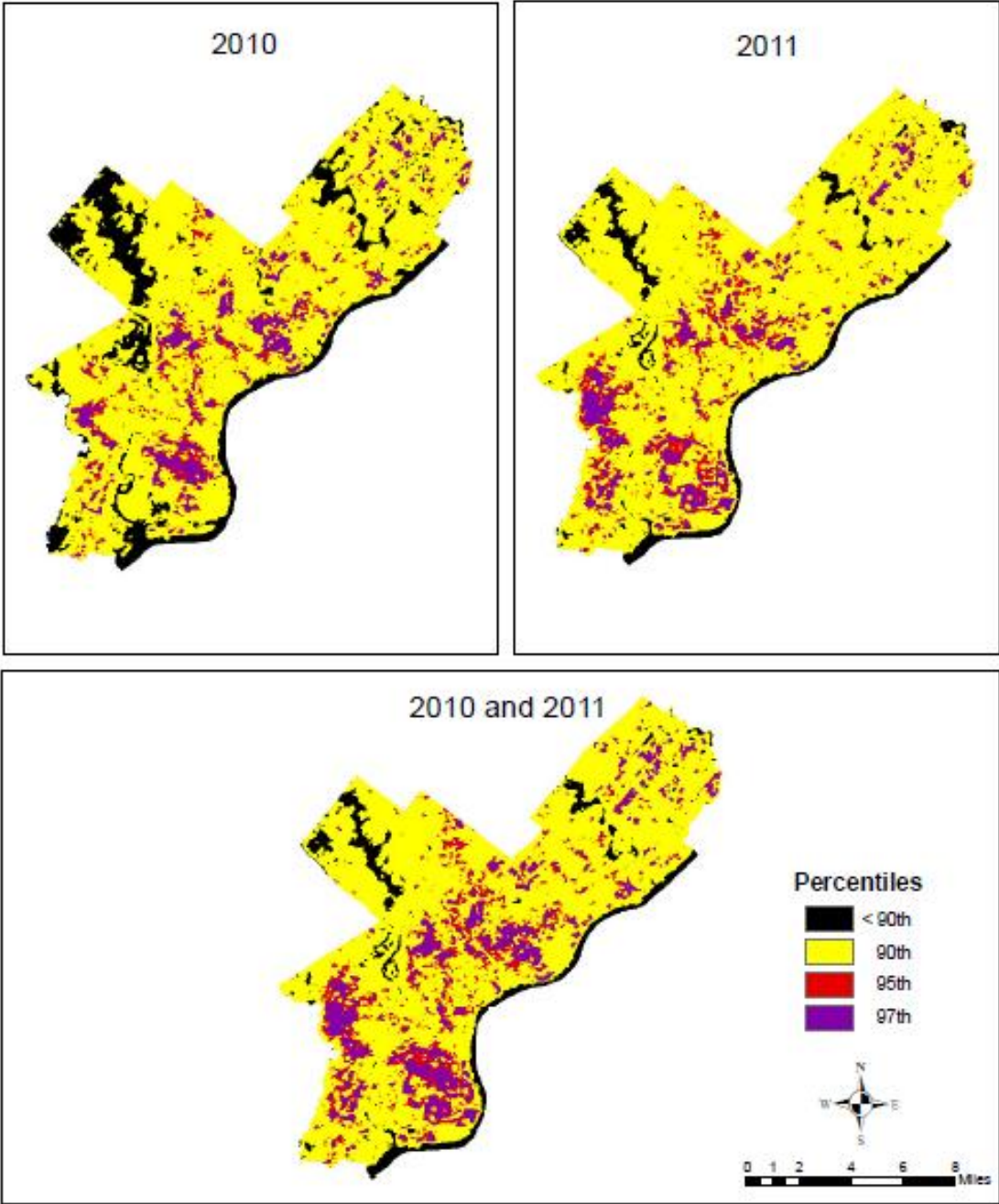Figure 23.A composite map showing percentile distribution of heat in Indianapolis

Figure 24.A composite map showing percentile distribution of heat in Philadelphia

## REFERENCES

Arnfield, A. J. (2003). "Two decades of urban climate research: a review of turbulence, exchanges of energy and water, and the urban heat island." <u>International Journal of Climatology</u> **23**(1): 1-26.

Cutter, S. L. and C. Finch (2008). "Temporal and spatial changes in social vulnerability to natural hazards." <u>Proceedings of the National Academy of Sciences of the United States of America</u> **105**(7): 2301-2306.

Davis, R. E., P. C. Knappenberger, et al. (2002). "Decadal changes in heat-related human mortality in the eastern United States." <u>Climate Research</u> **22**(2): 175-184.

Dousset, B. and F. Gourmelon (2003). "Satellite multi-sensor data analysis of urban surface temperatures and landcover." <u>ISPRS Journal of Photogrammetry and Remote Sensing</u> **58**(1): 43-54.

Ebi, K. L., T. J. Teisberg, et al. (2004). "Heat watch/warning systems save lives." <u>Bulletin of the American Meteorological Society</u> **85**(8): 1067-1073.

Gallo, K. P. and T. W. Owen (1999). "Satellite-based adjustments for the urban heat island temperature bias." <u>Journal of Applied Meteorology</u> **38**(6): 806-813.

Gallo, K. P., J. D. Tarpley, et al. (1995). "Assessment of Urban Heat Islands - a Satellite Perspective." <u>Atmospheric Research</u> **37**(1-3): 37-43.

Garcia-Cueto, O., E. Jauregui-Ostos, et al. (2007). "Detection of the urban heat island in Mexicali, BC, México and its relationship with land use." <u>Atmósfera</u> **20**(2): 111-131.

Harlan, S. L., A. J. Brazel, et al. (2006). "Neighborhood microclimates and vulnerability to heat stress." <u>Social Science & Medicine</u> **63**(11): 2847-2863.

Huang, C., Y. Shao, et al. (2008). <u>Temporal Analysis of Land Surface Temperature in Beijing Utilizing Remote Sensing Imagery</u>. Geoscience and Remote Sensing Symposium, 2008. IGARSS 2008. IEEE International, IEEE.

Johnson, D. P. and J. S. Wilson (2009). "The socio-spatial dynamics of extreme urban heat events: The case of heat-related deaths in Philadelphia." <u>Applied Geography</u> **29**(3): 419-434.

Johnson, D. P., J. S. Wilson, et al. (2009). "Socioeconomic indicators of heat-related health risk supplemented with remotely sensed data." <u>International Journal of Health Geographics</u> **8**.

Johnson, D.P., J.Webber, et al. (2013). "Spatiotemporal variations in heat-related risk in three midwestern U.S cities between 1990 and 2010." Geocarto International (in Press).

Kalkstein, L. S., P. F. Jamason, et al. (1996). "The Philadelphia hot weather-health watch/warning system: development and application, summer 1995." Bulletin of the American Meteorological Society **77**(7): 1519-1528.

Kestens, Y., A. Brand, et al. (2011). "Modelling the variation of land surface temperature as determinant of risk of heat-related health events." International Journal of Health Geographics **10**.

Liu, L. and Y. Zhang "Urban heat island analysis using the Landsat TM data and ASTER data: A case study in Hong Kong." Remote Sensing **3**(7): 1535-1552.

Lo, C. P., D. A. Quattrochi, et al. (1997). "Application of high-resolution thermal infrared remote sensing and GIS to assess the urban heat island effect." International Journal of Remote Sensing **18**(2): 287-304.

Markham, B. L. and J. Barker (1986). "Landsat MSS and TM post-calibration dynamic ranges, exoatmospheric reflectances and at-satellite temperatures." EOSAT Landsat technical notes **1**: 3-8.

Patz, J. A., M. A. McGeehin, et al. (2001). "The potential health impacts of climate variability and change for the United States - Executive summary of the report of the health sector of the US National Assessment." Journal of Environmental Health **64**(2): 20-28.

Qin, Z., A. Karnieli, et al. (2001). "A mono-window algorithm for retrieving land surface temperature from Landsat TM data and its application to the Israel-Egypt border region." International Journal of Remote Sensing **22**(18): 3719-3746.

Reid, C. E., M. S. O'Neill, et al. (2009). "Mapping Community Determinants of Heat Vulnerability." Environmental Health Perspectives **117**(11): 1730-1736.

Stanforth, A. C.(2011) Identifying Variations of Socio-spatial Vulnerability to Heat-related Mortality During the 1995 Extreme Heat Event in Chicago, IL, USA, faculty of the University Graduate School in partial fulfillment of the requirements for the degree Master of Science in the Department of Geography, Indiana University.

Stone, B., J. J. Hess, et al. (2010). "Urban Form and Extreme Heat Events: Are Sprawling Cities More Vulnerable to Climate Change Than Compact Cities?" Environmental Health Perspectives **118**(10): 1425-1428.

Tomlinson, C. J., L. Chapman, et al. (2011). "Including the urban heat island in spatial heat health risk assessment strategies: a case study for Birmingham, UK." International Journal of Health Geographics **10**.

Unger, J., Z. Sumeghy, et al. (2003). Cross-Section Profiles of the Urban Heat Island. Proc. of Fifth Int. Conf. on Urban Climate, Lodz, Poland.

Voogt, J. A. and T. R. Oke (2003). "Thermal remote sensing of urban climates." Remote Sensing of Environment **86**(3): 370-384.

Weng, Q. (2003). "Fractal analysis of satellite-detected urban heat island effect." Photogrammetric Engineering and Remote Sensing **69**(5): 555-566.

Xiao, R. B., Q. H. Weng, et al. (2008). "Land surface temperature variation and major factors in Beijing, China." Photogrammetric Engineering and Remote Sensing **74**(4): 451-461.

Yuan, F. and M. E. Bauer (2007). "Comparison of impervious surface area and normalized difference vegetation index as indicators of surface urban heat island effects in Landsat imagery." Remote Sensing of Environment **106**(3): 375-386.

Zhang, J. Q. and Y. P. Wang (2008). "Study of the Relationships between the Spatial Extent of Surface Urban Heat Islands and Urban Characteristic Factors Based on Landsat ETM plus Data." Sensors **8**(11): 7453-7468.

# CURRICULUM VITAE

Kavya Urs Beerval Ravichandra

## EDUCATION

Master of Science in Geographic Information Science, Indiana University-Purdue University Indianapolis
(August 2010 - July 2013)

Master of Science in Environmental Science, Bangalore University, India
(July 2003 - July 2005)

Bachelor of Science in Environmental Science, Bangalore University, India
(July 2000 - July 2003)

## RESEARCH AND TRAINING EXPERIENCE

Geographic Information Science Intern, the Polis Center, IUPUI, Indianapolis
(May 2012 - May 2013)
- Utilized LiDAR datasets for detecting and analyzing Levees in Indiana State.
- Created natural hazard models for disaster mitigation, planning and assessment for university campuses in Indiana.
- Created Hurricane and Flood models for Texas (TNRIS) using HAZUS ESRI extension, FME (Feature Manipulation Engine) scripts and CDMS building stock data import.
- Performed flood risk analysis by using FEMA approved ESRI extension and RiskMAP (Mapping, Assessing and Planning).
- Performed data editing, validation and map production by incorporating new Flood Hazard areas for the counties of Indiana.
- Worked with the Polis Center GIS Analysts and Indiana Department of Natural Resources (IDNR) to resolve mapping issues

Graduate Research Assistant, Department of Geography, Indiana University, Indianapolis
(January 2011 - May 2012)
- Developed qualitative and quantitative methods to estimate the spatial patterns of extreme heat events using geospatial data.
- Analyzed land use and land cover patterns using Landsat Thematic Mapper data.
- Measured social variables by statistical analysis using SPSS.

Service Learning Assistant, Department of Geography, Indiana University, Indianapolis
(August 2010 - May 2011)
- Assisted Dr. Frederick L. Bein in coursework for undergraduates.
- Assisted in grading and evaluation of the semester quizzes and projects.
- Delivered lecture on Biodiversity.

## PROFESSIONAL EXPERIENCE

CITIZENS ENERGY GROUP, Indianapolis
(Anticipated start date - July 2013)
Geographic Information Science Intern/Analyst


ACCENTURE TECHNOLOGY SERVICES Pvt. Ltd., Bangalore, India
(October 2006 - December 2009)
Senior Process Analyst –Pharmaceutical Health and Life Sciences
- Served as a project point of contact for technical shared services providing detailed setup and configuration knowledge and expertise.
- As a client liaison, coordinated the projects between the software programmers and clients, including building and execution of protocols.
- Managed and coordinated the delivery of technical aspects of Electronic Data Capture trials for leading pharmaceutical companies using Oracle based Phase Forward Inform EDC software.
- Built Electronic Case Report Forms using Oracle based Inform (Phase Forward) platform, RAVE and Visual Basic (VB).


MOUNT CARMEL COLLEGE, BANGALORE UNIVERSITY, Bangalore, India
(July 2005 - October 2005)
Part-time lecturer
- Delivered lectures on environmental management, environmental pollution, energy management, wildlife conservation, environmental resources and environmental impact assessment.
- Graded papers

## PUBLICATIONS

Monitoring of forest fires in Bhadra Wildlife Sanctuary
Journal: Indian Society of Remote Sensing
March 2008, Volume 36, Issue 1, pp. 99-104

Spatiotemporal variations in heat-related risk in three Midwestern U.S cities between 1990 and 2010.
Journal: Geocarto International
2013 In press